Passive Droplet Control in Two-Dimensional Microfluidic Networks

Gerold Fink, *Student Member, IEEE,* Medina Hamidović, *Student Member, IEEE,*
Robert Wille, *Member, IEEE,* and Werner Haselmayr, *Member, IEEE*

***Abstract*—Microfluidic networks for droplet-based microfluidics have been recently introduced with the aim of realizing flexible Lab-on-Chip devices. In this paper, we investigate, for the first time, a two-dimensional network topology, in which biological samples, embodied in so-called payload droplets, are delivered to a specific destination. Two-dimensional networks can be useful in many applications, such as the automation of laboratory experiments on microwell plates. The path of the payload droplet is determined by the network geometry and the distance to so-called control droplets (i.e., passive droplet control). In order to route single or multiple payload droplets to a specific destination, we introduce droplet frames that include single or multiple payload droplets and several control droplets for their path control. We derive closed-form expressions for the droplet distances within the frame to realize the desired droplet routing. These expressions are solely based on the network geometry and fluid properties. Computer simulations based on the analogy between microfluidic networks and electrical circuits verified the proposed routing scheme.**

***Index Terms*—Droplet-based microfluidics, lab-on-chip**

I. Introduction

Molecular communication (MC) is an emerging field that broadly defines information transmission using molecules and provides the basis for various future healthcare applications [1]. In recent years, most of the research has been devoted to diffusive MC, where the information-bearing molecules are subject to Brownian motion [1]. However, since diffusion is a very slow process, such systems suffer from high attenuation and delay. This limitation can be overcome by exploiting fluid flow, which is present in many envisioned MC environments, such as blood vessels and microfluidic chips. In [2], [3], [4], [5], [6], [7], concentration propagation models were presented where the information-bearing molecules are dispersed into a continuous fluid flowing in microchannels. Instead of concentration of molecules, droplets that flow in an immiscible continuous fluid have been proposed for information transmission in [8]. Various information encoding schemes and the corresponding achievable information rates have been presented for such droplet-based microfluidic systems [9], [10], [11]. Moreover, this approach paves the way for new computing and networking paradigms, since the droplets can be independently controlled [8], [12].

Microfluidic networks are microfluidic systems that interconnect multiple microfluidic devices (e.g., mixing, sorting) on a single microfluidic chip [8]. The aim of droplet-based networking is to deliver biological samples, embodied in the droplet, to a specific destination in the network [8], [9], [13], [14]. Moreover, in order to keep the microfluidic chip as simple as possible no active control of the droplets using micro-valves or externally applied forces is used. Instead, the droplet's path is controlled by only exploiting passive hydrodynamic principles. This approach is an important step towards the next generation of Lab-on-Chip (LoC) devices, enabling more flexibility, bio-compatibility and low-cost fabrication [15], [16]. In order to realize the passive droplet control, two key elements are required: microfluidic switches and addressing schemes.

Microfluidic switches make it possible to control the path of the droplets containing biological samples by using an additional droplet that contains no biological samples. Following the information and communications technology (ICT) terminology, we refer to the former as payload and to the latter as control droplet. Two different types of microfluidic switches have been proposed so far: i) Single-Droplet-Switches (SDS) control the path of a single payload droplet using a single control droplet [9]; ii) Multi-Droplet-Switches (MDS) control the path of multiple payload droplets using only a single control droplet [17].

The addressing scheme drives the switching process at a bifurcation. For example, in size-based switching [18] the size of the control droplet changes the switching behavior, while in distance-based switching [13] the payload path is controlled by its distance to the control droplet. It is important to note that in droplet-based networking we distinguish between two types of information. Biological information that is included in the payload droplets, and digital information that corresponds to the destination address and is included either in the control droplets size or in the distance between control and payload droplets.

Based on the aforementioned switching devices and addressing schemes, three different topologies have been proposed for microfluidic networks so far: i) ring networks can be used to route a single payload droplet through the network and enables to execute the operations of multiple microfluidic devices in a row [9], [14], [19]; ii) application-specific architectures are designed for a pre-defined set of experiments to be conducted and are able to deliver a single payload droplet to a single or multiple microfluidic devices [20]; iii) bus networks can guide single and multiple payload droplets to a specific destination [13], [17]. The bus topology offers the highest flexibility and scalability and enables parallel processing of payload droplets.

However, there are various practical scenarios where the one-dimensional (1D) bus network proposed in [13], [17] is not suitable. For example, a microfluidic chip with a

microfluidic network structure mounted on a microwell plate can be used to automatically deliver biological samples to the individual wells. In this case, due to the typical arrangement of the wells on the microwell plate, it is preferable to use a microfluidic network with a two-dimensional (2D) topology. Another potential application would be a DNA-based archival storage system [21], [22]. This paper extends the investigations on 1D bus networks [13], [17] to 2D-networks. In particular, this paper, for the first time, investigates passive control of single and multiple payload droplets in a 2D-network. The main contributions of this paper can be summarized as follows:

- We propose a 2D microfluidic network in which single or multiple payload droplets can be delivered to a specific destination.
- We propose a novel droplet frame that consists of single or multiple payload droplets and the corresponding control droplets for their path control.
- We derive closed-form analytical expressions for the droplets' distances within the droplet frame to enable the desired routing.
- We verify the proposed addressing schemes through a recently proposed simulation tool for microfluidic networks [23], [24], which is based on the analogy between microfluidic and electrical circuits.

The rest of the paper is organized as follows: In Section II, we introduce the physical model of droplet-based microfluidic systems. The principles of Single- and Multi-Droplet-Switches are presented in Section III. In Section IV, the addressing scheme for the path control of a single and multiple payload droplets in the 2D-network is introduced. The validation of the droplet routing is validated by computer simulations in SectionV. Finally, Section VI provides concluding remarks.

II. Physical Model

In order to design a 2D-network, specific flow rates inside the network must satisfy certain conditions, which are derived in later sections. Therefore, a physical model is required, which describes the behavior of microfluidic systems. To this end, the one-dimensional (1D) analysis model proposed in [25], [26] can be utilized. This model assumes that pumps produce a fully developed and laminar flow (usually at low Reynolds numbers) – a property which is satisfied in the case considered here. Then, the flow inside a channel can be described by Hagen-Poiseuille's law [27] as

$$\Delta P = Q \cdot R \ , \tag{1}$$

where Q is the volumetric flow rate, ΔP the pressure drop along the channel, and R the hydrodynamic resistance of the channel. This hydrodynamic resistance depends on the channel geometry (i.e., length l, width w, and height h) as well as the dynamic viscosity of the continuous phase μ_c. More precisely, for rectangular channels with a section ratio $h/w < 1$, the hydrodynamic resistance can be determined by [28]

$$R = \frac{a\mu_\mathrm{c} l}{wh^3} \ , \tag{2}$$

where a denotes a dimensionless parameter defined as

$$a = 12\left[1 - \frac{192h}{\pi^5 w}\tanh\left(\frac{\pi w}{2h}\right)\right]^{-1} \ . \tag{3}$$

Moreover, droplets also increase the resistance of a channel. As proposed in [29], a droplet with the length l_Droplet increases the resistance of the segment it occupies inside the channel by $2-5$ times. As a rule of thumb, we will use the factor 3 in this work, i.e.,

$$R_\mathrm{Droplet} = \frac{3a\mu_\mathrm{c} l_\mathrm{Droplet}}{wh^3} \ . \tag{4}$$

This 1D analysis model can now be used to describe the behavior of a microfluidic network. In order to realize this, the channels of such networks can be represented by their hydrodynamic resistances, which leads to the so-called equivalent electrical network [25][1]. This equivalent electrical network can then be used to compute the volumetric flow rates inside the channels.

III. Building Blocks

As described above, a 2D-network is used to route one or more payload droplets towards a specific destination, which is usually a particular output channel of the network. Moreover, it should be controllable towards which destination these droplets are routed. Therefore, special building blocks are required, which are able to guide droplets towards a desired path – a so-called microfluidic switch. With these building blocks it is then possible to build a complete 2D-network. In the following we discuss such building blocks in more detail and derive conditions which are important for the construction of a 2D-network.

A. Single-Droplet-Switch

The first building block we are investigating is the so-called Single-Droplet-Switch (SDS), which refers to a T-Junction with bypass channel and is shown in Fig. 1. The first idea of this concept was proposed in [30] and was later improved by [31] [18]. As Fig. 1 illustrates, a SDS consists of one input channel and two output channels (*Out1* and *Out2*), where the two output channels are additionally connected by the bypass channel *By*. This bypass channel cannot be entered by droplets, due to the barriers at the entrances of the bypass channel, and is used to make the switching mechanism of the SDS more stable [32].

A single droplet which flows inside the input channel and reaches the bifurcation point B_1, is always routed towards the channel with the lowest hydrodynamic resistance, or in other words, with the highest instantaneous flow rate. Since a SDS is designed in such a way that the volumetric flow rate of channel *In1* is larger than the flow rate of channel *In2*, i.e., $Q_\mathrm{In1} > Q_\mathrm{In2}$, the droplet is routed through the channel *In1* towards the channel *Out1* (cf. Fig. 2a). This path is also called the default path, whereas the path towards channel *Out2* is called the non-default path. As described in

[1]It is called equivalent electrical network, because the representation is equivalent to an electrical resistor network.

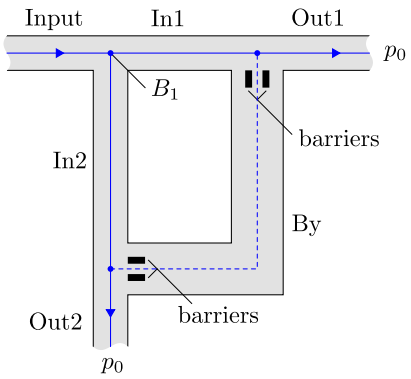

Fig. 1. Design of a Single-Droplet-Switch

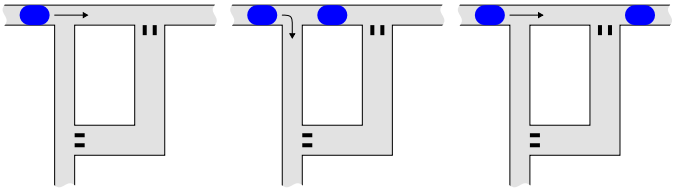

Fig. 2. Droplet path control inside a SDS based on hydrodynamic principles.

Section II, a droplet increases the hydrodynamic resistance of the channel it occupies (cf. (4)). Hence, when a droplet is present inside the channel *In1* it increases the channel's hydrodynamic resistance, so that the channel's volumetric flow rate is now lower than the flow rate of channel *In2*. In other words, the condition $Q_{\text{In1}}^{(\text{In1})} < Q_{\text{In2}}^{(\text{In1})}$ now holds, where the superscript indicates, that a droplet is present inside the channel *In1*. Therefore, a second droplet closely following the first one is guided towards the channel *Out2* (cf. Fig. 2b), i.e., into the non-default path. In contrast, if the distance between the two droplets was so large, that the first droplet is already in the output channel *Out1* when the second droplet arrives at the bifurcation point, then $Q_{\text{In1}} > Q_{\text{In2}}$ holds again and the second droplet follows the first one into the default path (cf. Fig. 2c).

As a result, this switching mechanism allows to define the path of the second droplet, only by controlling the distance between the two droplets before they reach the SDS. Since only the path of the second droplet can be controlled, it is usually a payload droplet, while the first droplet is a control droplet, which is only used for addressing purposes.

1) Switching Conditions: In order to realize the correct behavior of the SDS, certain conditions need to be satisfied, otherwise the switching mechanism would not work. As already mentioned, the volumetric flow rates are crucial for the correct behavior of the SDS. These volumetric flow rates can be determined by applying the 1D-model on the design of the SDS (cf. Fig. 1), resulting in the equivalent electrical network shown in Fig. 3. With this equivalent electrical network it is then possible to obtain the required volumetric flow rate inside a channel, by applying Kirchhoff's current and voltage law. More precisely, we determine the normalized volumetric flow rate, which describes the flow rate inside a channel normalized to the flow rate of the input channel, Q_{Input}. Hence, a normalized volumetric flow rate is a dimensionless parameter, where the absolute value of the flow rate can always be obtained, by multiplying the normalized flow rate with the flow rate of the input channel Q_{Input}. For the channel *In1*, this normalized volumetric flow rate can be computed as follows

$$q_{\text{In1}} = \frac{Q_{\text{In1}}}{Q_{\text{Input}}} = \frac{R_{\text{By}}\left(R_{\text{In2}} + R_{\text{Out2}}\right) + R_{\text{In2}}\tilde{R}_{\text{Out}}}{R_{\text{By}}\left(\tilde{R}_{\text{In}} + \tilde{R}_{\text{Out}}\right) + \tilde{R}_{\text{In}}\tilde{R}_{\text{Out}}} \ , \tag{5}$$

where the hydrodynamic resistances $\tilde{R}_{\text{In}}$ and $\tilde{R}_{\text{Out}}$ can be expressed as

$$\tilde{R}_{\text{In}} = R_{\text{In1}} + R_{\text{In2}} \ , \quad \tilde{R}_{\text{Out}} = R_{\text{Out1}} + R_{\text{Out2}} \ . \tag{6}$$

As described before, a single droplet which flows towards the bifurcation point B_1 should be routed into the channel *In1* and, thus, $q_{\text{In1}} > q_{\text{In2}}$ must hold. By considering Kirchhoff's current law, i.e., $Q_{\text{Input}} = Q_{\text{In1}} + Q_{\text{In2}} \rightarrow 1 = q_{\text{In1}} + q_{\text{In2}}$, this condition can be reformulated as

$$q_{\text{In1}} > 0.5 \ , \tag{7}$$

and represents the first condition which has to be satisfied, in order to get a correct working SDS. That is, the normalized volumetric flow rate q_{In1} has to be greater than 0.5. In the following, we call this specific state of the switch, where no droplet is present inside the channel *In1*, the OFF-State.

When a droplet occupies the channel *In1*, a second droplet closely following the first one, should be routed into the non-default path, i.e., the condition $q_{\text{In1}}^{(\text{In1})} < q_{\text{In2}}^{(\text{In1})}$ must hold, where the superscript indicates that the additional hydrodynamic resistance of the droplet has to be considered inside the channel *In1*. Hence, the normalized volumetric flow rate $q_{\text{In1}}^{(\text{In1})}$ can be computed identically to (5), but R_{In1} has to be substituted by $R_{\text{In1}} \rightarrow R_{\text{In1}} + R_{\text{Droplet}}$. Again, due to Kirchhoff's current law, this condition can be reformulated and yielding the second condition to be satisfied

$$q_{\text{In1}}^{(\text{In1})} < 0.5 \ . \tag{8}$$

This state, where a droplet is present in the channel *In1*, is called the ON-State of the switch. Moreover, in the remainder of this work, we use the term "triggered" in order to indicate, that the state of the switch changed from the OFF- to the ON-State.

Overall, when the conditions in (7), and (8) are fulfilled, the SDS satisfies the desired switching behavior.

2) Droplet Distances: If two droplets flow towards a SDS, the distance between them decides if the second droplet is routed into the default or non-default path. More precisely, if the distance is shorter than a specific threshold d_{ON}, the first droplet is still present inside the channel *In1* (i.e., the switch is in the ON-State) when the second droplet arrives at the switch and, thus, the second droplet is routed into the non-default path (cf. Fig. 2b). In contrast, the switch is not triggered (i.e. the switch is in the OFF-Sate), when the distance is longer than the threshold d_{OFF} and, therefore, the second droplet follows

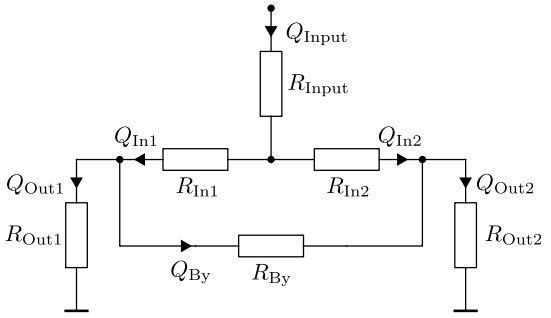

Fig. 3. Equivalent electrical network of a SDS

the first one into the default path (cf. Fig. 2c). These two thresholds can be determined by the equations (cf. App. VII-A)

$$d_{\text{ON}} = \frac{1}{q_{\text{In1}}^{(\text{In1})}} \left(l_{\text{In1}} - l_{\text{Droplet}}\right) + l_{\text{Droplet}} \quad \text{and} \tag{9}$$

$$d_{\text{OFF}} = \frac{1}{q_{\text{In1}}^{(\text{In1})}} l_{\text{In1}} + l_{\text{Droplet}} \ , \tag{10}$$

where l_{In1} and l_{Droplet} are the lengths of the channel *In1* and the droplet, respectively. Note that, if the actual droplet distance lies between the thresholds d_{ON} and d_{OFF}, it is hard to predict which path the second droplet takes. This is due to the fact, that in this case the first droplet lies neither completely in the channel *In1* nor in the channel *Out1* when the second droplet reaches the bifurcation point B_1. As a result, it cannot be predicted if the flow rate of channel *In1* is larger or smaller than the flow rate inside the channel *In2* and, thus, it is not possible to safely determine the path of the second droplet. Hence, droplet distances which lie in this particular range should be avoided.

Overall, the second droplet can be routed into the default or non-default path, when the distance between the first and second droplet (in the following denoted by d) satisfies $d > d_{\text{OFF}}$ or $d < d_{\text{ON}}$, respectively.

3) Droplet Distance Reduction: An important characteristic of a SDS is, that the distance between two droplets changes, when they pass a SDS and are routed into the same output channel. More precisely, the distance between these two droplets after the SDS is shorter than the distance before the SDS. This is due to the fact, that the volumetric flow rate of the continuous phase (coming from the input channel) splits into the two output channels. Hence, a part of the continuous phase between the droplets flows into the other output channel, which reduces the volume of the continuous phase between the droplets and, thus, reduces the distance of the two droplets. When both droplets flow towards the output channel *Out1*, i.e., the default path, this distance reduction can be described by the reduction factor r_1 $(r_1 < 1)$

$$d^{(1)} = r_1 \ d^{(2)} \ , \tag{11}$$

where $d^{(1)}$ and $d^{(2)}$ are the distances before and after the SDS, respectively. The exact value of the reduction factor r_1 depends on the ratio between the volumetric flow rate of the output channel *Out1* and the input channel, or in other words on the normalized volumetric flow rate q_{Out1}, which can be calculated as

$$r_1 = q_{\text{Out1}} = \frac{R_{\text{By}} \left(R_{\text{In2}} + R_{\text{Out2}}\right) + R_{\text{Out2}} \tilde{R}_{\text{In}}}{R_{\text{By}} \left(\tilde{R}_{\text{In}} + \tilde{R}_{\text{Out}}\right) + \tilde{R}_{\text{In}} \tilde{R}_{\text{Out}}} \ . \tag{12}$$

Similar to the reduction factor for the output channel *Out1*, it is also possible to define the reduction factor for the output channel *Out2*

$$r_2 = q_{\text{Out2}} = 1 - q_{\text{Out1}} \ , \tag{13}$$

where Kirchhoff's current law ($q_{\text{Out1}} + q_{\text{Out2}} = 1$) was utilized again. For a detailed derivation of the two reduction factors, please see App. VII-B. The reduction factors become very important when multiple SDSs are connected within a network, as described in Section IV.

B. Multi-Droplet-Switches

In this section, we describe the so-called Multi-Droplet-Switch (MDS), which was first proposed in [17]. In this work, we will consider a slightly modified version, that simplifies the analysis. More precisely, we omitted the bypass channel in the control region of the original design, which was initially used to increase the time the switch stays in a particular state. In this state, the switch is able to route a droplet towards an output channel which is usually not the default path (similar to a SDS). While the adapted design makes many derivations far easier, it is more sensitive against uncertainties of the switching distance, i.e., the distance the droplets must have in order to activate the switching mechanism. However, the obtained droplet distances can also be applied to the original design and, thus, it is recommended to use the original design during the fabrication process, since it reduces these sensitivity issues.

In comparison to the SDS, the MDS can route multiple payload droplets into a desired output channel only with the use of one control droplet. This means, while a SDS always has an overhead of 50%, the overhead of a MDS gets reduced with each additional payload droplet and, thus, allows for a much higher throughput [17].

The design of the MDS, shown in Fig. 4, consists of a control and a switching region. These two regions are connected by the channel *C1* and the control channel *Ctrl*, where only channel *C1* can be passed by a droplet. This is due to the geometrical constraints of the MDS design, which does not allow a droplet to enter the control channel *Ctrl*.

Control region: As the name indicates, this region is used to control the flow rate of the control channel *Ctrl*. If we assume a droplet is present at the bifurcation point B_1, then the entrance of the control channel *Ctrl* is blocked (cf. Fig. 5b). As a result, the continuous phase cannot flow into the channel *Ctrl* and the flow rate q_{Ctrl} becomes zero. We call this special condition, the ON-State. In the OFF-State on the other hand, no droplet blocks the entrance to the control channel *Ctrl* (cf. Fig. 5b) and, thus, the continuous phase flows into the channel.

Switching region: In the switching region the droplet is routed into the desired output channel. The destination of the

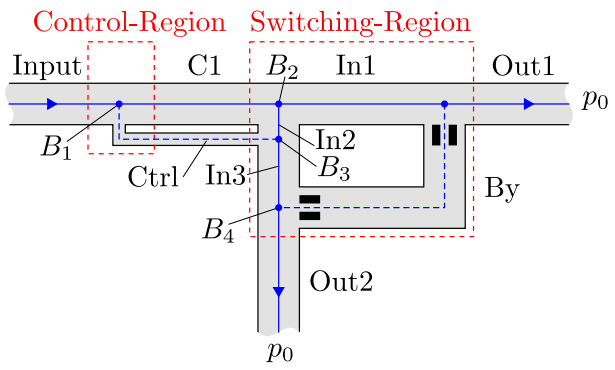

Fig. 4. Design of a Multi-Droplet-Switch.

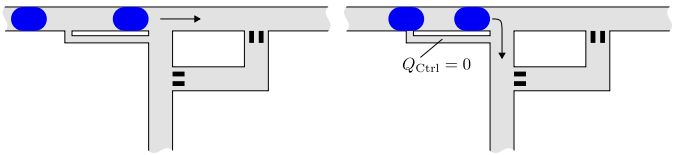

(a) OFF-State (b) ON-State

Fig. 5. Droplet gets routed into different output channels.

droplet depends on the current state (i.e., ON- or OFF-State), when it reaches the bifurcation point B_2. In the ON-State, the switching region has basically the same structure as a SDS. At the point B_2 the channel *C1* splits into two branches, where the branch between B_2 and B_4, i.e., *In2* and *In3*, has a lower hydrodynamic resistance than channel *In1*, i.e., the channel is shorter. Therefore, the flow rate q_{In1} is smaller than the flow rates of q_{In2} and q_{In3}. Hence, if a droplet reaches the point B_2 during the ON-State, it is routed through the channels *In2* and *In3* towards the output channel *Out2*. In the OFF-State there is still a flow rate entering the switching region at point B_3. With an appropriate design of the MDS it is possible to obtain a flow rate of the *Ctrl* channel, which changes the condition of the flow rates to $q_{\text{In1}} > q_{\text{In2}}$. As a result, a droplet arriving at the bifurcation point B_2 gets directed through the channel *In1* towards the output channel *Out1*.

If a droplet should be routed into the output channel *Out2*, a droplet must block the channel *Ctrl*, otherwise it gets directed into the output channel *Out1*. To accomplish this, the two droplets must have an appropriate distance before they arrive at the MDS. If we now assume that we inject multiple droplets into the input channel, which all have this appropriate distance, then each droplet is routed into the output channel *Out2*, because the control channel *Ctrl* always gets blocked by the previous droplet. However, the last droplet will be directed into the channel *Out1*, because it has no other droplet which blocks the channel *Ctrl*. Therefore, the last droplet always has to be a control droplet, if all payload droplets should be routed into the output channel *Out2*.

1) Switching Conditions: Similar to Section III-A1, certain conditions have to be satisfied, in order to get a MDS which works as described above. Again, the normalized volumetric flow rates inside the channels play an important role and can be obtained by applying the 1D-model on the design of

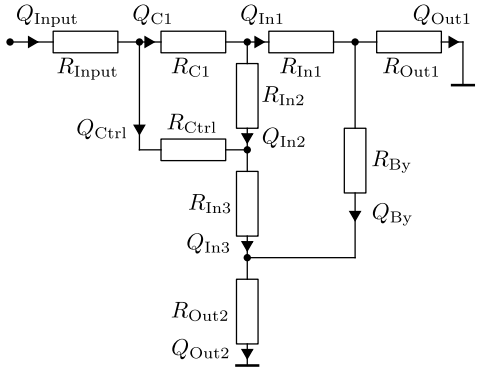

Fig. 6. Equivalent electrical network of a MDS.

the MDS (cf. Fig. 4), resulting in the equivalent electrical network shown in Fig. 6. In order to compute the normalized volumetric flow rates in the channels during the OFF-State, Kirchhoff's current and voltage laws can be utilized, resulting in the following linear equation system

$$\mathbf{A}_{\text{OFF}}\ \mathbf{q} = \mathbf{b}\ , \tag{14}$$

with the matrix

$$\mathbf{A}_{\text{OFF}} = \begin{bmatrix} 1 & 1 & 0 & 0 & 0 & 0 & 0 & 0 \\ 1 & 0 & 1 & -1 & 0 & 0 & 0 & 0 \\ 0 & 1 & -1 & 0 & -1 & 0 & 0 & 0 \\ 0 & 0 & 0 & 1 & 0 & 1 & -1 & 0 \\ 0 & 0 & 0 & 0 & 1 & -1 & 0 & -1 \\ R_{\text{Ctrl}} & -R_{\text{C1}} & -R_{\text{In2}} & 0 & 0 & 0 & 0 & 0 \\ 0 & 0 & R_{\text{In2}} & R_{\text{In3}} & -R_{\text{In1}} & -R_{\text{By}} & 0 & 0 \\ 0 & 0 & 0 & 0 & 0 & R_{\text{By}} & R_{\text{Out2}} & -R_{\text{Out1}} \end{bmatrix} \tag{15}$$

and the vector

$$\mathbf{b}^\top = \begin{bmatrix} 1 & 0 & 0 & 0 & 0 & 0 & 0 & 0 \end{bmatrix}\ . \tag{16}$$

When solving the equation system (14) the vector $\mathbf{q}$ contains the normalized volumetric flow rates

$$\mathbf{q}^\top = \begin{bmatrix} q_{\text{Ctrl}} & q_{\text{C1}} & q_{\text{In2}} & q_{\text{In3}} & q_{\text{In1}} & q_{\text{By}} & q_{\text{Out2}} & q_{\text{Out1}} \end{bmatrix}\ . \tag{17}$$

A droplet, which flows towards the bifurcation point B_2 during the OFF-State, should be routed into the channel *In1*. Hence, the volumetric flow rate of channel *In1* must be larger than the flow rate of channel *In2*, resulting in the first condition which has to be satisfied in order to realize the correct behavior of a MDS

$$q_{\text{In1}}^{(\text{C1}),\,\text{OFF}} > q_{\text{In2}}^{(\text{C1}),\,\text{OFF}}\ , \tag{18}$$

where the superscript *C1* indicates, that a droplet is present inside the channel *C1*. Hence, when computing these flow rates, the resistance R_{C1} in the matrix (15) must be substituted by $R_{\text{C1}} \rightarrow R_{\text{C1}} + R_{\text{Droplet}}$.

During the ON-State a droplet blocks the entrance of the control channel *Ctrl* at the bifurcation point B_1 and, thus, the volumetric flow rate inside the control channel becomes zero. In the equivalent electrical network (cf. Fig. 6) this can be considered by removing the resistance R_{Ctrl} or in other words, by setting the value of R_{Ctrl} against infinity. Therefore, the normalized volumetric flow rates in the ON-State can be

computed using (14) and replacing $\mathbf{A}_{\text{OFF}}$ by $\mathbf{A}_{\text{ON}}$, which is defined by

$$\mathbf{A}_{\text{ON}} = \begin{bmatrix} 0 & 1 & 0 & 0 & 0 & 0 & 0 & 0 \\ 0 & 0 & 1 & -1 & 0 & 0 & 0 & 0 \\ 0 & 1 & -1 & 0 & -1 & 0 & 0 & 0 \\ 0 & 0 & 0 & 1 & 0 & 1 & -1 & 0 \\ 0 & 0 & 0 & 0 & 1 & -1 & 0 & -1 \\ 1 & 0 & 0 & 0 & 0 & 0 & 0 & 0 \\ 0 & 0 & R_{\text{In2}} & R_{\text{In3}} & -R_{\text{In1}} & -R_{\text{By}} & 0 & 0 \\ 0 & 0 & 0 & 0 & 0 & R_{\text{By}} & R_{\text{Out2}} & -R_{\text{Out1}} \end{bmatrix} . \quad (19)$$

When a droplet flows towards the bifurcation point B_2 during the ON-State, it should be routed into the channel *In2*. Therefore, the flow rate of channel *In1* must be smaller than the flow rate of channel *In2* this time, i.e., $q_{\text{In1}}^{\text{ON}} < q_{\text{In2}}^{\text{ON}}$, yielding the second condition which has to be satisfied in order to get a MDS which works as expected. Since the flow rate of the control channel is zero, Kirchhoff's current law ($q_{\text{In1}}^{\text{ON}} + q_{\text{In2}}^{\text{ON}} = 1$) can be utilized to reformulate the condition

$$q_{\text{In1}}^{\text{ON}} < 0.5 . \quad (20)$$

Overall, the conditions (18) and (20) have to be satisfied, in order to get a MDS realizing the correct behavior.

2) Droplet Distances: When two droplets arrive at a MDS, the distance d between these droplets decides, if the switching process of the MDS is triggered or not. That is, when d lies between the thresholds $d_{\text{ON,min}} < d < d_{\text{ON,max}}$, the switching process of the MDS is triggered and therefore, the first droplet is routed into the output channel *Out2*. If the switching process should not be triggered, so both droplets flow towards the channel *Out1*, the distance must be longer than the threshold d_{OFF}. For an appropriate design of a MDS the following condition always holds

$$d_{\text{ON,min}} < d_{\text{ON,max}} < d_{\text{OFF}} . \quad (21)$$

The thresholds can be computed as follows, where the detailed derivation of the thresholds can be found in App. VII-A.

$$d_{\text{ON,min}} = \frac{1}{q_{\text{C1}}^{(\text{C1}),\,\text{OFF}}} \left(l_{\text{C1}} - 2l_{\text{Droplet}}\right) + l_{\text{Droplet}} \quad (22)$$

$$d_{\text{ON,max}} = \frac{1}{q_{\text{C1}}^{(\text{C1}),\,\text{OFF}}} \left(l_{\text{C1}} - l_{\text{Droplet}}\right) + l_{\text{Droplet}} \quad (23)$$

$$d_{\text{OFF}} = \frac{l_{\text{C1}}}{q_{\text{C1}}^{(\text{C1}),\,\text{OFF}}} + \frac{l_{\text{In1}}}{q_{\text{In1}}^{(\text{In1}),\,\text{OFF}}} + l_{\text{Droplet}} . \quad (24)$$

Again, the superscript indicates, that a droplet is present in the corresponding channel, e.g., the normalized volumetric flow rate $q_{\text{In1}}^{(\text{In1}),\,\text{OFF}}$ has to be computed by substituting the resistance R_{In1} in the matrix $\mathbf{A}_{\text{OFF}}$ with $R_{\text{In1}} \rightarrow R_{\text{In1}} + R_{\text{Droplet}}$.

The MDS is designed in such a way, that it only works properly, when the distance between the droplets d lies in a particular range, i.e., $d_{\text{ON,min}} < d < d_{\text{ON,max}}$ and $d_{\text{OFF}} < d$. However, if the droplet distance is shorter than $d_{\text{ON,min}}$ or lies between the thresholds $d_{\text{ON,max}}$ and d_{OFF} it is hard to predict in which output channel the two droplets will flow. This is due to the complexity of the MDS, since the flow rates inside the channels depend on many factors, such as the position of the droplets or the channel geometries, which affect the droplet paths. Hence, distances which do not lie in the specified range of the thresholds should be avoided, when the MDS should work as expected.

3) Droplet Distance Reduction: If two droplets flow towards a MDS and the switching process is not triggered (OFF-State), both droplets are routed into the output channel *Out1*. Similar to the droplet distance reduction of a SDS, the distance of these droplets before and after the MDS is not identical. This is because the volume of the continuous phase between the droplets gets smaller, since a part of the volume flows into the output channel *Out2* (cf. Section III-A3). The distance reduction can be calculated exactly the same way as for the SDS in (11). Hence, the reduction factor is the ratio between the volumetric flow rate of the output channel *Out1* and the input channel or in other words, the normalized volumetric flow rate q_{Out1}

$$r_1 = q_{\text{Out1}}^{\text{OFF}} , \quad (25)$$

which can be computed by solving (14).

IV. 2D-Network

Basically, microfluidic 2D-networks are networks, which consist of a single input channel and multiple output channels, which lead the payload droplets towards a specific destination. The network in Fig. 7 shows the general design of such a 2D-network with a 2×3 structure, where the first number indicates the amount of branches in the network, and the second number specifies the amount of output channels in each branch. Therefore this 2D-network has $2 \times 3 = 6$ output channels, which are denoted by $Out_{i,j}$, where i is the index of the branch and j the index of the output channel of the branch. The other output channels are connected to the reservoir and are used to collect the control droplets. Hence, only payload droplets and no control droplets are routed into the output channels $Out_{i,j}$. As indicated in Fig. 7, each branch consists of several switches in a row (denoted by $\text{S}_{i,j}$), where all switches are either SDSs or MDSs. Moreover, each branch is connected to an output channel of another SDS. These SDSs form the so-called splitter, since it divides the input channel into several branches. If the switches of the branches consist of SDSs we call the network a Single-Payload-Droplet-Network, which can only handle one payload droplet per addressing process. Otherwise, the network is called a Multi-Payload-Droplet-Network, if the branches only consist of MDSs. Such a network is able to route multiple payload droplets during an addressing process to a single output channel.

A. 1D-Network

As we can see in Fig. 7, the splitter as well as the branches consist of several switches in a row and, thus, form a one-dimensional (1D) or bus network. Therefore, we will first discuss the properties and the addressing process of such a 1D-network as shown in Fig. 9, before we discuss the 2D-network. The switches in the 1D-network only consists of either SDSs or MDSs and, thus, each switch is characterized by the parameters d_{OFF}, r_1, d_{ON} (SDS), and d_{OFF}, r_1, $d_{\text{ON,min}}$, and $d_{\text{ON,max}}$ (MDS), which were derived in Secs. III-A and III-B. Furthermore, we assume, that these parameter values are identical for all switches.

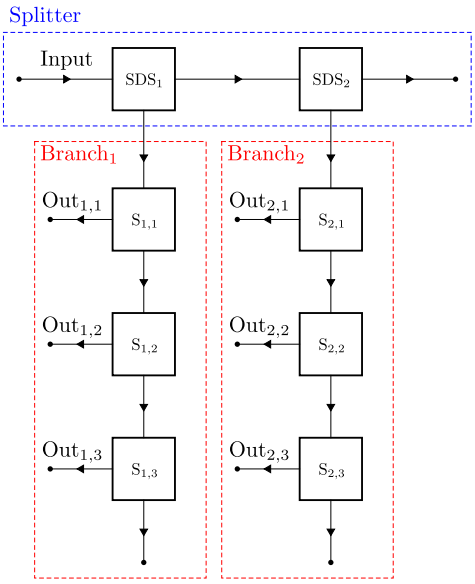

Fig. 7. Basic structure of a 2D-network with 2 branches and 3 output channels in each branch.

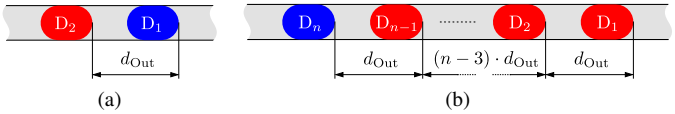

Fig. 8. Droplet frame which is needed to address a desired output channel in the 1D-network shown in Fig. 9, where all the switches in the network consists either of (a) SDSs or (b) MDSs. Blue indicates control droplets and red payload droplets.

1) Addressing Scheme & Droplet Frame: When a single payload droplet should be routed into a particular output channel of the 1D-network then the network only consists of SDSs, and the droplet frame illustrated in Fig. 8a must be injected into the input channel of the network. In contrast, when multiple payload droplets should be routed into one output channel, the network only consists of MDSs and the droplet frame shown in Fig. 8b must be used.

Once the droplet frame is injected into the input channel of the network, the droplets flow towards the first switch. Unless the output channel of the first switch should be addressed, the droplets pass this switch without triggering its switching mechanism. However, when they pass the switch, their distance reduces accordingly to the reduction factor (12) or (25) (cf. Fig. 9). This happens at each passed switch, until their distance has an appropriate length in order to trigger the switching process of the next switch. Hence, the distance between the droplets d_{Out} at the input channel (cf. Fig. 8a and Fig. 8b) decides which switch is addressed and, thus, into which output channel of the 1D-network the payload droplets are routed. The derivation of the required distance d_{Out} is discussed next.

2) Droplet Distance Computation: In order to compute the correct droplet distance d_{Out} of the droplet frames at the input channel, we assume, that the i^{th} output channel of the 1D-network, i.e., Out_i, should be addressed (cf. Fig. 9). Therefore, the switching mechanism of the i^{th} switch S_i must

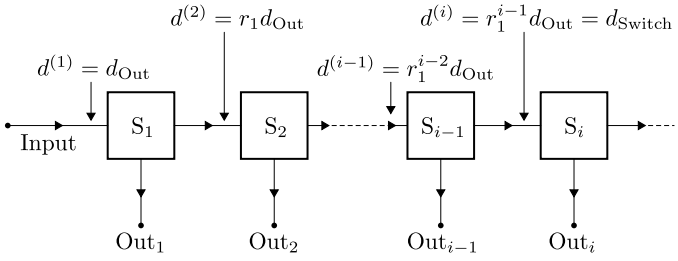

Fig. 9. Basic structure of a 1D network.

be triggered, which is only possible if the droplet distance $d^{(i)}$ in front of the i^{th} switch has an appropriate value. We refer to this special distance as switching distance

$$d^{(i)} = d_{\text{Switch}} \ . \tag{26}$$

If two droplets pass the $(i-1)^{\text{th}}$ switch, their distance before the switch $d^{(i-1)}$ is longer than the distance after the switch $d^{(i)}$ according to the reduction factor r_1

$$d^{(i)} = r_1 \ d^{(i-1)} \ . \tag{27}$$

Hence, when utilizing (27) recursively, the droplet distance $d^{(1)} = d_{\text{Out}}$ at the input channel can be easily computed with respect to the switching distance and yields (cf. Fig. 9)

$$d^{(1)} = d_{\text{Out}} = \frac{d_{\text{Switch}}}{r_1^{i-1}} \ . \tag{28}$$

The switching distance d_{Switch} depends on the used switches in the network, i.e., SDSs or MDSs. Hence, in a 1D-network, which only consists of MDSs, the switching distance d_{Switch} before the i^{th} MDS can be computed as follows

$$d_{\text{Switch}} = \frac{d_{\text{ON,min}} + d_{\text{ON,max}}}{2} \ . \tag{29}$$

Please note, that the thresholds $d_{\text{ON,min}}$ and $d_{\text{ON,max}}$ are minimal and maximal limits, which should not be exceeded and, thus, the "optimal" switching distance for a MDS is the mean value of these two thresholds. The output channel of the i^{th} switch can only be addressed, if the switching mechanism of the $(i-1)^{\text{th}}$ switch is not triggered, which yields the following condition for d_{Switch}

$$d_{\text{OFF}} < d^{(i-1)} \overset{(26),\ (27)}{\longrightarrow} d_{\text{OFF}} \ r_1 < d_{\text{Switch}} \ . \tag{30}$$

As a result, a 1D-network, solely consisting of MDSs, must be designed in such a way, that

$$d_{\text{OFF}} \ r_1 < \frac{d_{\text{ON,min}} + d_{\text{ON,max}}}{2} \tag{31}$$

is fulfilled. If this is not the case, the network would not work as intended, because not all output channels of the switches would be addressable—in fact only the first switch could be addressed, since it has no previous switch.

For a 1D-network, which only consists of SDSs, the switching distance d_{Switch} before the i^{th} SDS must be smaller than d_{ON} (cf. Section III-A2). Again, d_{Switch} must be large enough, that the switching mechanism of the $(i-1)^{\text{th}}$ switch is not triggered, yielding

$$d_{\text{OFF}} \ r_1 < d_{\text{Switch}} < d_{\text{ON}} \ . \tag{32}$$

However, (32) also implies, that an appropriate droplet distance can only exist, when the network is designed in such a way, that

$$d_{\text{OFF}}\ r_1 < d_{\text{ON}} \tag{33}$$

is satisfied. As described before, the network would not work properly, if this condition is not satisfied. Since the thresholds d_{ON}, and d_{OFF} are minimal or maximal limits, which should not be exceeded, a good choice for the switching distance can be determined by

$$d_{\text{Switch}} = \frac{d_{\text{ON}} + d_{\text{OFF}}\ r_1}{2}\ . \tag{34}$$

Overall, when designing a 1D-network, the designer has to make sure, that (31) or (33) is fulfilled for a network which only consists of MDSs or SDSs, respectively. Afterwards, the switching distance d_{Switch} can be computed for MDSs or SDSs, according to (29) or (34), respectively. Finally, the droplet distance d_{Out} at the input channel can be obtained with (28), in order to address the i^{th} output channel of the network.

B. Single-Payload-Droplet-Network

The Single-Payload-Droplet-Network (SPDN) only consists of SDSs and is able to route a single payload droplet per addressing process into a specific output channel of the network.

1) Addressing Scheme & Droplet Frame: In order to route a payload droplet into a specific output channel of the network, the droplet frame shown in Fig. 10 has to be injected into the input channel of the SPDN, which consists of four droplets. As the figure illustrates, the first three droplets of this frame are control droplets, while the last one (D_4) is the payload droplet, which should be routed into the corresponding output channel. Moreover, the frame consists of two smaller droplet pairs, namely *Pair*$_1$ (droplets D_1 and D_2) and *Pair*$_2$ (droplets D_3 and D_4). Each of these pairs is used to route the respective second droplet (droplets D_2 and D_4) into the desired branch. Since the splitter is a 1D-network, the addressing scheme of each droplet pair is identical to the scheme described in Section IV-A1, i.e., the initial droplet distance gets reduced with every passed SDS, until the switching mechanism of the correct SDS is triggered. Therefore, the addressed branch can be controlled with the distance between the droplets inside the droplet pairs, i.e., d_{Branch}. Once the droplets D_2 and D_4 are in the correct branch, they have a certain droplet distance, which depends on the distance d_{Out} between the two droplet pairs at the input channel. This droplet distance inside the actual branch now decides which output channel of the branch is addressed, which, again, works identical to the addressing scheme of a 1D-network. Hence, with the distance between the droplet pairs d_{Out} it is possible to control which output channel of the branch is addressed and, thus, in which channel the payload droplet D_4 is routed. In other words, the addressing scheme of the SPDN (or a 2D-network in general) is in principle the cascading of the addressing scheme of two 1D-networks. Of course, the distances d_{Branch} and d_{Out} must be chosen in such a way, that the correct output channel is addressed. How to accomplish this is described next.

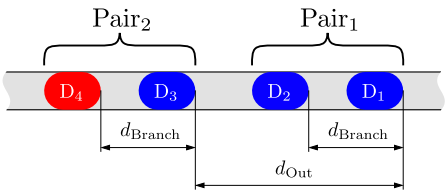

Fig. 10. Droplet frame which is needed to address a desired output channel in a SPDN. Blue indicates control droplets and red payload droplets.

2) Computation of Droplet Distances: The addressing scheme of a 2D-network is basically the addressing scheme of two 1D-networks in a row. Therefore, we can utilize the results derived in Section IV-A2 in order to compute the required droplet distances d_{Branch} and d_{Out} of the droplet frame shown in Fig. 10. To accomplish this, we assume that we want to address the j^{th} output channel inside the i^{th} branch, i.e., $Out_{i,j}$.

First, we want to derive the distance d_{Branch} inside the droplet pairs, which controls the addressed branch. Since the splitter is a 1D-network consisting of SDSs, the distance d_{Branch} at the input channel of the network can be easily computed by combining (34) and (28), which yields

$$d_{\text{Branch}} = \frac{d_{\text{ON}} + d_{\text{OFF}}\ r_{1,S}}{2} \frac{1}{(r_{1,S})^{i-1}}\ , \tag{35}$$

where $r_{1,S}$ indicates the reduction factor of the SDSs inside the splitter. Hence, d_{Branch} is the "optimal" switching length of a SDS enlarged by the reduction factors r_1 of the switches, which have to be passed by the droplets.

In order to derive the distance d_{Out}, we first compute the droplet distance d^*_{Out} (between the droplets D_2 and D_4) at the beginning of the branch, which is required to route the payload droplet into the j^{th} output channel. Since the branch is also a 1D-network consisting of SDSs, the distance can be derived identical to (35), where $r_{1,B}$ indicates the reduction factor of the SDSs inside the branches this time

$$d^*_{\text{Out}} = \frac{d_{\text{ON}} + d_{\text{OFF}}\ r_{1,B}}{2} \frac{1}{(r_{1,B})^{j-1}}\ . \tag{36}$$

The next step is to use d^*_{Out} and compute the required distance d_{Out} at the input channel of the network. Again, this can be achieved similar to (35), since the splitter is a 1D-network consisting of SDSs. However, we have to consider, that the droplets D_2 and D_4 pass the i^{th} SDS of the splitter through the non-default path and, thus, an additional distance reduction of the two droplets must be considered by the reduction factor r_2 (cf. Section III-A3)

$$\begin{aligned} d_{\text{Out}} &= \frac{d^*_{\text{Out}}}{r_{2,S}\ (r_{1,S})^{i-1}} \\ &= \frac{d_{\text{ON}} + d_{\text{OFF}}\ r_{1,B}}{2} \frac{1}{r_{2,S}\ (r_{1,S})^{i-1}\ (r_{1,B})^{j-1}}\ . \end{aligned} \tag{37}$$

The expression (37) seems reasonable, since the "optimal" distance between the droplets D_2 and D_4 is enlarged by the reduction factors of the switches they pass, i.e., the first $(i-1)$ SDSs of the splitter through the default path, the i^{th} SDS of the splitter through the non-default path and finally the first $(j-1)$ SDSs of the i^{th} branch through the default path.

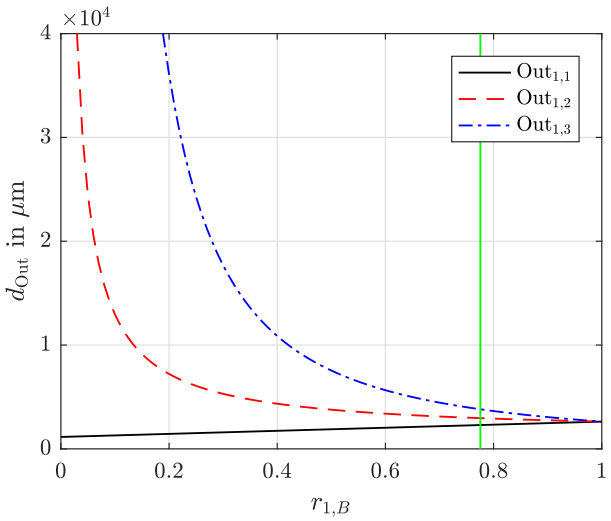

Fig. 11. Required droplet distance d_{Out} for each output channel of the first branch as a function of the reduction factor $r_{1,B}$. Please note, that only values with $r_{1,B} < 0.78$ (green line) are possible, since the design criterion (33) has to be satisfied.

How the droplet distance d_{Out} depends on the reduction factor $r_{1,B}$ can be seen in Fig. 11. For this purpose, the other parameters in (37) are set to proper constant values, namely $r_{1,S} = r_{2,S} = 0.5$, $d_{\text{ON}} = 1147\,\mu\text{m}$ and $d_{\text{OFF}} = 1479\,\mu\text{m}$ (these values are taken from the SPDN discussed in Section V-C). Moreover, Fig. 11 illustrates the corresponding distance for the first three output channels ($j = 1, 2, 3$) inside the first branch ($i = 1$) of a SPDN with a 2×3 structure (cf. Fig. 7). It can be observed that, besides the droplet distance for the first output channel $Out_{1,1}$, the distance increases with a lower reduction factor, where the rate of growth of each curve depends on the corresponding index of the output channel. Since a smaller droplet distance d_{Out} means higher throughput of the droplets, the network should be designed in such a way, that the reduction factor $r_{1,B}$ is not too small. The droplet distance for the first output channel $Out_{1,1}$ is nearly constant, because the droplets do not have to pass the first switch in the branch when this output channel is addressed and, thus, d_{Out} does not have to be enlarged by the reduction factor of the first switch. Please note, that not all values for the reduction factor would result in a working network, since also the design criterion (33) has to be satisfied, i.e., only values with $r_{1,B} < \frac{d_{\text{ON}}}{d_{\text{OFF}}} = 0.78$ are possible as indicated in Fig.11.

C. Multi-Payload-Droplet-Network

In contrast to the SPDN, the branches of the Multi-Payload-Droplet-Network (MPDN) consist only of MDSs and, thus, it is possible to route multiple payload droplets per addressing process into a specific output channel of the network.

1) Addressing Scheme & Droplet Frame: We first want to discuss the addressing scheme and the needed droplet frame, when several payload droplets should be routed into a specific output channel. Fortunately, the addressing scheme of the MPDN share many similarities with the addressing scheme of the SPDN. The required droplet frame is shown in Fig. 12, which consists of N droplets, where every second

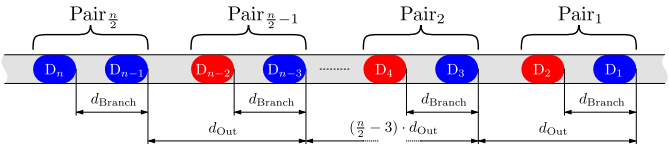

Fig. 12. Droplet frame at the input channel of a MPDN. Blue indicates control droplets and red payload droplets.

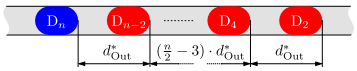

Fig. 13. Droplet frame inside a branch of a MPDN. Blue indicates control droplets and red payload droplets.

droplet is a payload droplet, except the last one, which is a control droplet like the rest of the droplets. Furthermore, the frame consists of $N/2$ droplet pairs, where each pair is a combination of a control and payload droplet, except the last pair, which solely consists of control droplets. Identical to the addressing scheme of the SPDN, each droplet pair is used to route the respective second droplet into the desired branch. As a result, the distance between the droplets inside the droplet pairs, i.e., d_{Branch}, controls which branch is addressed. Once every second droplet is in the correct branch, they form a new droplet frame shown in Fig. 13, where the distance between two adjacent droplets is always the same and depends on the distance d_{Out} between the droplet pairs at the input channel. Since a single branch of a MPDN only consists of MDSs, the addressing scheme of such branch is identical to the addressing scheme of a 1D-network with MDSs (cf. Section IV-A1). Hence, the distance between the droplets in the new droplet frame decides which output channel of the actual branch is addressed. Therefore, the distance d_{Out} between the droplet pairs at the input channel, controls which output channel of the branch is addressed and, thus, in which channel the payload droplets are routed. Again, the distances d_{Branch} and d_{Out} must be chosen in such a way, that the correct output channel is addressed. The detailed derivation of these distances is described next.

2) Computation of Droplet Distances: Since the addressing scheme of a MPDN is still an addressing scheme of two 1D-networks in a row, we can derive the correct droplet distances d_{Branch} and d_{Out} of the droplet frame shown in Fig. 12 similar to the derivation we did for the SPDN in Section IV-B.

The only difference is, that the branches of a MPDN solely consists of MDSs. Hence, we have to utilize the derivations from Section IV-A2, in order to get the correct droplet distances d_{Branch} and d_{Out}. Again, we assume that the j^{th} output channel inside the i^{th} branch should be addressed, i.e., $Out_{i,j}$.

Because the splitters of a SPDN and MPDN are identical, the distance d_{Branch} inside the droplet pairs, which controls the addressed branch, can also be computed identical, i.e., (35) must be used.

Similar to Section IV-B, we first derive the droplet distance d^*_{Out} (cf. Fig. 13) at the beginning of the branch, which is required to route the payload droplet into the j^{th} output channel. This time we have to consider, that the branches are 1D-networks solely consisting of MDSs. Thus, we have to

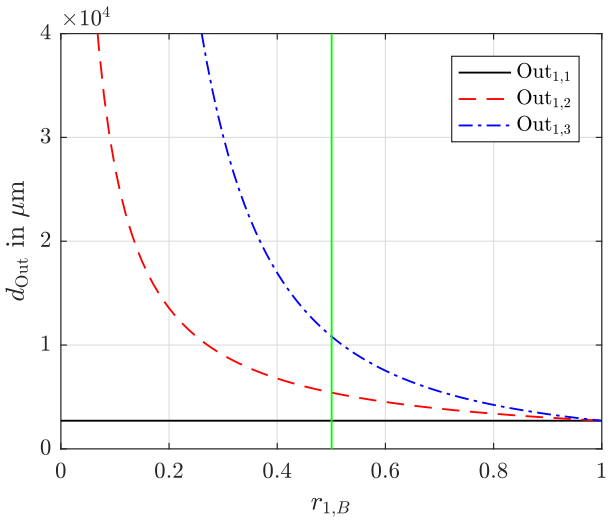

Fig. 14. Required droplet distance d_{Out} for each output channel of the first branch as a function of the reduction factor $r_{1,B}$. Please note, that only values with $r_{1,B} < 0.5$ (green line) are possible, since the design criterion (31) has to be satisfied.

combine (28) with the "optimal" switching distance of a MDS represented by (29), which yields

$$d^*_{\text{Out}} = \frac{d_{\text{ON,min}} + d_{\text{ON,max}}}{2} \frac{1}{(r_{1,B})^{j-1}} \ . \tag{38}$$

Now we can derive the required distance d_{Out} at the input channel of the network identical to Section IV-B. Again, we have to consider that all droplets inside the branch pass the i^{th} SDS of the splitter through the non-default path and, thus, the distance reduction of the droplets must be considered by the reduction factor r_2 (cf. Section III-A3)

$$\begin{aligned} d_{\text{Out}} &= \frac{d^*_{\text{Out}}}{r_{2,S}\ (r_{1,S})^{i-1}} \\ &= \frac{d_{\text{ON,min}} + d_{\text{ON,max}}}{2} \frac{1}{r_{2,S}\ (r_{1,S})^{i-1} (r_{1,B})^{j-1}} \ . \end{aligned} \tag{39}$$

Similar to the SPDN, Fig. 14 illustrates the droplet distance d_{Out} as a function of the reduction factor $r_{1,B}$. To this end, all other parameters in (39) are set to proper constant values, namely $r_{1,S} = r_{2,S} = 0.5$, $d_{\text{ON,min}} = 1239\,\mu\text{m}$ and $d_{\text{ON,max}} = 1472\,\mu\text{m}$ (these values are taken from the MPDN discussed in Section V-D). Again, the figure shows the corresponding distance for the first three output channels ($j = 1, 2, 3$) and the first branch ($i = 1$) of a MPDN with a 2×3 structure (cf. Fig. 7). While the droplet distance for the first output channel $Out_{1,1}$ is constant, the distance becomes larger with lower values for the reduction factor and also increases faster with a higher index of the corresponding output channel. Hence, for smaller values of the distance d_{Out} and, thus, for higher throughput of the droplets, the reduction factor $r_{1,B}$ should not be too small. Please note, that not all values for the reduction factor would be possible, since the design criterion (31) must also be fulfilled, i.e., when assuming $d_{\text{OFF}} = 2707\,\mu\text{m}$ then only values for $r_{1,B} < \frac{d_{\text{ON}}}{d_{\text{OFF}}} = 0.5$ are suitable as indicated in Fig. 14.

Overall, in order to design a 2D-network which works as intended, all aforementioned design conditions for the network/switches have to be satisfied and the correct droplet distances for a particular output channel must be accordingly computed. However, if these conditions are violated or the droplet distances are not properly chosen, then the network would not work as expected.

For example, when the design conditions (7) and (8) for SDSs or (18) and (20) for MDSs are not satisfied, then the network would not work at all, because the switches would lose their ability to route droplets towards different paths. On the other hand, when only the design conditions (31) and (33) for cascaded switches in a 1D-network are violated, then not all output channels of the network would be addressable (or in the worst case, not even a single output channel at all), regardless of the applied droplet distances at the input channel.

If all design conditions for the network/switches are fulfilled, but the correct droplet distances are not properly chosen, then the droplets would be routed towards a wrong output channel. The severity of this failure would depend on the individual application of the network and might be negligible or could even destroy the whole experiment.

V. Simulation & Validation

In order to validate the concept of the addressing scheme and its derivations for the required droplet distances, we simulate a SPDN and a MPDN in the following. In particular, we first provide a brief overview on the simulation process and then define the initial simulation setup as well as the channel dimensions of the two networks. Based on these values, we determine the required droplet distances with the derivations made in the previous sections, in order to route payload droplets into particular output channels of the networks. A guideline which summarizes the required design steps is shown in Fig. 15.

A. Simulator

In order to make this work self contained, we will briefly discuss the working principles of the utilized simulator proposed in [24]. However, for a more detailed explanation we refer to [24] and [33]. The simulator is based on the 1D-analysis model described in Section II and captures the behavior of a microfluidic network in the following five steps:

1) *Initialization:* Before the actual simulation can start, the designer has to initialize the simulator first, i.e., specifications such as the used fluids, the dimensions of the channels, etc. have to be defined. After the initialization, the simulator basically performs the following steps in a loop, until a termination conditions is reached.
2) *Compute flow state:* Based on the equivalent hydrodynamic resistances of the channels and droplets of the network, the simulator establishes a linear equation system. Afterwards, the equations system is solved in order to determine the instantaneous flow state (i.e. pressure drops and flow rates in all channels) inside the microfluidic network. This flow state allows to compute

Generating the Network Design:

- Define initial parameters:
  - Used fluids
  - Channel width and height
  - Droplet volume/length
  - Volumetric flow rate of the pump
  - Structure of the 2D-network (amount of branches and output channels)
- Determine the dimensions of the switches/network, while considering the corresponding design conditions
  - For SDSs: (7) and (8)
  - For MDSs: (18) and (20)
  - For cascaded SDSs: (33)
  - For cascaded MDSs: (31)

Generating Droplet Sequences:

- Compute the required droplet distances for each output channel
  - For a SPDN: (37)
  - For a MPDN: (39)

Fig. 15. Guidelines for designing a 2D-network and determining the corresponding droplet distances.

the velocities of the droplets, which are required in the next step.

3) *Compute next event-time:* The previously obtained droplet velocities allow to determine at which time the next event is happening. Such an event basically happens, when the current flow state of the microfluidic network changes and can be triggered for example by
   - injecting a new droplet into the network,
   - a droplet flowing into another channel, or
   - a droplet leaving the network.
4) *Update system state:* The simulator updates the system state (i.e. droplet positions and their resistances in the channels) accordingly to the occurred events. Here the droplet velocities and the time interval between the current and last event are used to update the position of all droplets.
5) *Termination condition:* If a termination condition is reached (e.g., all droplets left the network), the simulation stops, otherwise, the simulator continues with Step 2 and computes the flow state again.

Overall, after initializing the simulator, it always re-calculates the flow state of the network, when the old one becomes invalid due to an occurrence of an event and accordingly updates the droplet positions and the corresponding channel resistances. This allows to trace the droplet paths and, thus, the behavior of the microfluidic network.

B. Simulation Setup

Before we are able to simulate a network, we first have to define some basic parameters, like the fluid properties, pressure/flow rate of the pump, etc. (cf. Table I). Additionally, we assume that these parameters are the same for both networks. The parameters μ_c and μ_d indicate the dynamic viscosities of the continuous and dispersed phase, respectively. Furthermore, we assume, that each input channel of the two networks has a constant volumetric flow rate, which is given by the parameter Q_{Input}. Another important value is the volume of the droplets, which is the same for all droplets and is indicated by the parameter V_{Droplet}. Moreover, we define that all channels inside the networks have the same height h and that all channels, which can be passed by a droplet, have a width of w. As a result, the length of the droplets can be computed by $l_{\text{Droplet}} = V_{\text{Droplet}}/(w\ h)$. Please note, that the parameters used in Table I represent a common setup for microfluidic devices, for example parameters in a similar range have been used in [9], [34]. However, it is important to note that of course also other simulation parameters can be applied. For a properly working network only the conditions established throughout this work must hold.

TABLE I
SIMULATION PARAMETERS

μ_c	μ_d	Q_{Input}	V_{Droplet}	h	w	l_{Droplet}
mPa s	mPa s	µL min^{-1}	µL	µm	µm	µm
1	4	2.15	0.000495	33	100	150

TABLE II
CHANNEL DIMENSIONS IN µm OF THE SDSs INSIDE THE SPLITTER.

	l_{In1}	l_{In2}	l_{Out1}	l_{Out2}	w_{By}
SDS_1	300	490	3396	3000	150
SDS_2	300	490	7139	3000	150
$\text{SDS}_{1,1}$, $\text{SDS}_{1,2}$	600	800	4000	7418	150
$\text{SDS}_{2,1}$, $\text{SDS}_{2,2}$	600	800	4000	6255	150
$\text{SDS}_{3,1}$, $\text{SDS}_{3,2}$	600	800	4000	3927	150

Once we defined the simulation parameters, we can now define the geometry of the two networks.

C. Single-Payload-Droplet-Network

In order to obtain the required droplet distances at the input channel and to simulate the SPDN, we have to define the structure and the channel dimensions of the network. Therefore, we assume that the SPDN has a 2×3 structure like the 2D-network in Fig. 7, i.e., 2 branches and 3 output channels per branch. All channel dimensions of the SDSs in the splitter and the SDSs in the branches can be found in Table II. Moreover, Table III represents all parameters of the switches, which are relevant for the computation of the correct droplet distances (cf. Section III-A). The table also shows that the switching conditions (7) and (8) as well as the condition for an appropriate design (33) are satisfied. Please note, that the dimensions of the switches (cf. Table II) are choosen in such a way, that all switches in the splitter and all switches in the branches have the same parameters, as shown in Table III.

With these parameters it is now possible to obtain the required droplet distances of the droplet frame shown in Fig. 10, i.e., d_{Branch} and d_{Out}, according to (35) and (37). The resulting distances for each branch and output channel are summarized in Table IV.

TABLE III
PARAMETERS OF THE SDSS USED IN THE SPDN, WITH $i = \{1, 2\}$ AND $j = \{1, 2, 3\}$.

	q_{In1}	$q_{\text{In1}}^{(\text{In1})}$	r_1	r_2	d_{ON} (µm)	d_{OFF} (µm)
SDS_i	0.578	0.421	0.5	0.5	507	863
$\text{SDS}_{i,j}$	0.546	0.451	0.5	0.5	1147	1479

TABLE IV
DROPLET DISTANCES d_{BRANCH} AND d_{OUT} IN µm.

		$i = 1$	$i = 2$
d_{Branch}:	Branch_i	469	938
d_{Out}:	$\text{Out}_{i,1}$	1887	3773
	$\text{Out}_{i,2}$	3773	7547
	$\text{Out}_{i,3}$	7547	15094

In order to validate the addressing scheme and the obtained distances, we simulate the case, where the second output channel of the second branch gets addressed, i.e., $Out_{2,2}$. According to Table IV the droplet frame shown in Fig. 10 has to be injected into the input channel of the network with the distances $d_{\text{Branch}} = 938\,\mu\text{m}$ and $d_{\text{Out}} = 7547\,\mu\text{m}$.

The derived parameters are now fed to the simulator proposed in [24]. A video of the simulation results can be found here https://www.youtube.com/watch?v=vwl30E6pYkc, which demonstrates, that the addressing scheme works as proposed and that the presented droplet distance computation is correct.

Moreover, a screenshot of the simulation is illustrated in Fig. 16, which shows the SPDN with the corresponding SDSs and output channels. The screenshot captured the moment, where the header droplet D_2 and the payload droplet D_4 have already been routed into the correct branch through the two header droplets D_1 and D_3, respectively. Therefore, the droplets D_2 and D_4 currently have a distance of d_{Out}^* according to (36) and will both flow through the $\text{SDS}_{2,1}$ towards the $\text{SDS}_{2,2}$, where the switching mechanism gets triggered and where the payload droplet D_4 gets routed into the desired output channel $\text{Out}_{2,2}$.

Please note, that the channel dimensions of the switches in Table II are chosen in such a way, that the proposed addressing scheme can be easily validated. More precisely, these small dimensions allow to smoothly monitor the paths of the droplets as well as the switching processes in the network during the simulation video. However, the lengths of the channels could be easily adapted to meet the requirements of a practical use case, e.g., microfluidic chip with a 2D-network that is able to distribute droplets on a microwell plate. This can be done by adapting the lengths of the channels *Out1* and *Out2* of each switch, while the lengths of the channels *In1* and *In2* can remain the same. When also the same droplet distances (cf. Table IV) should be used to address the corresponding output channels, then it only has to be ensured, that the lengths of these channels are adapted in such a way, that the reduction factors r_1 and r_2 stay the same.

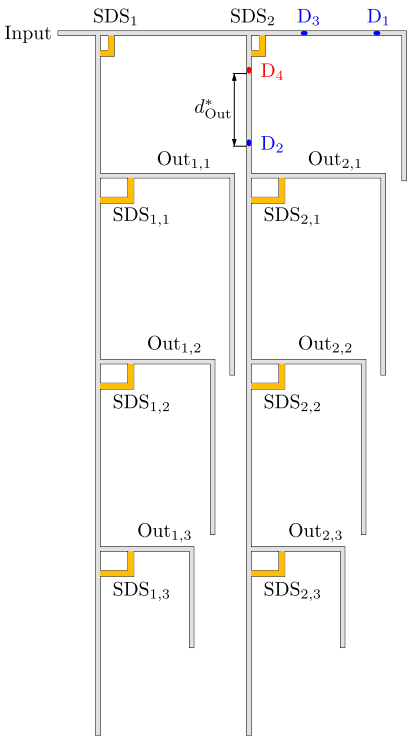

Fig. 16. Simulation screenshot of the SPDN.

TABLE V
CHANNEL DIMENSIONS IN µm OF THE SDSS INSIDE THE SPLITTER.

	l_{In1}	l_{In2}	l_{Out1}	l_{Out2}	w_{By}
SDS_1	300	490	6206	6000	150
SDS_2	300	490	12760	6000	150

D. Multi-Payload-Droplet-Network

For the MPDN we, again, assume that the network has a 2×3 structure, i.e., 2 branches and 3 output channels per branch. The channel dimensions of the SDSs in the splitter and the MDSs in the branches are shown in Table V and Table VI, respectively. The MPDN is designed in such a way, that the SDSs in the splitter have the same parameters as the ones from the splitter of the SPDN, and, thus can be, again, found in Table III. The parameters of the MDSs are represented in Table VII, where it can be seen, that the switching conditions (18) and (20) as well as the condition for an appropriate design (31) are satisfied. Please note, that the dimensions of the MDSs (cf. Table VI) are chosen in such a way, that the parameters of all the MDSs are identical, as shown in Table VII.

Again, we can utilize these parameters in order to obtain the required droplet distances of the droplet frame shown in Fig. 12, i.e., d_{Branch} and d_{Out}, according to (35) and (39). The resulting distances for each branch and output channel are presented in Table VIII. As it can be seen, the droplet distances for each branch d_{Branch} are identical to the one in the SPDN, since all parameters of the SDSs in the splitter are also the same.

As in Section V-C, we validate the addressing scheme and the obtained distances, for the case, where the second output

TABLE VI
CHANNEL DIMENSIONS IN µm OF THE MDSs IN THE BRANCHES.

	l_{C1}	l_{In1}	l_{In2}	l_{In3}	l_{Out1}	l_{Out2}	w_{Ctrl}	w_{By}
$MDS_{1,1}$	1000	250	100	100	6000	11771	50	150
$MDS_{1,2}$	1000	250	100	100	6000	11771	50	150
$MDS_{2,1}$	1000	250	100	100	6000	9859	50	150
$MDS_{2,2}$	1000	250	100	100	6000	9859	50	150
$MDS_{3,1}$	1000	250	100	100	6000	6034	50	150
$MDS_{3,2}$	1000	250	100	100	6000	6034	50	150

TABLE VII
PARAMETERS OF ALL MDSs IN THE MPDN.

$q_{In1}^{(C1),OFF}$	$q_{In2}^{(C1),OFF}$	q_1^{ON}	r_1	$d_{ON,min}$	$d_{ON,max}$	d_{OFF}
0.42	0.3	0.46	0.5	1239	1472	2707

channel of the second branch gets addressed, i.e., $Out_{2,2}$. Hence, the droplet frame shown in Fig. 12 has to be injected into the input channel of the network with the distances $d_{Branch} = 938\,\mu m$ and $d_{Out} = 10\,846\,\mu m$, accordingly to Table VIII. As an example we want to route 5 payload droplets into the output channel and, thus, we have to inject 6 droplet pairs respectively 12 droplets into the input channel (cf. Fig. 12).

A video of the simulation results can be found here https://www.youtube.com/watch?v=SGv9t2PRToU, which confirms, that the addressing scheme of the MPDN works as expected and that the computation of the droplet distances were correct.

Furthermore, Fig. 17 shows a simulation screenshot of the MPDN with the corresponding switches and output channels. The screenshot illustrates the moment, where the payload droplets D_2, D_4, D_6, and D_8 have already been routed into the second branch, while the payload droplet D_{10} and the header droplet D_{12} are still in the splitter and will be routed into the second branch by the header droplets D_9 and D_{11}, respectively. All payload droplets and the header droplet D_{12} will pass the $MDS_{2,1}$ and will flow towards the $MDS_{2,2}$, where the payload droplets will then be routed into the desired output channel $Out_{2,2}$.

Similar to the SPDN, the channel dimensions of the switches in Table V and Table VI are chosen in such a way, that the switching processes in the network can be easily observed in the simulation video. Nevertheless, the channel lengths can be easily adapted to fulfill the requirements of practical uses cases, e.g., for microwell plates.

TABLE VIII
DROPLET DISTANCES d_{BRANCH} AND d_{OUT} IN µm.

		$i=1$	$i=2$
d_{Branch}:	$Branch_i$	469	938
d_{Out}:	$Out_{i,1}$	2711	5423
	$Out_{i,2}$	5423	10846
	$Out_{i,3}$	10846	21691

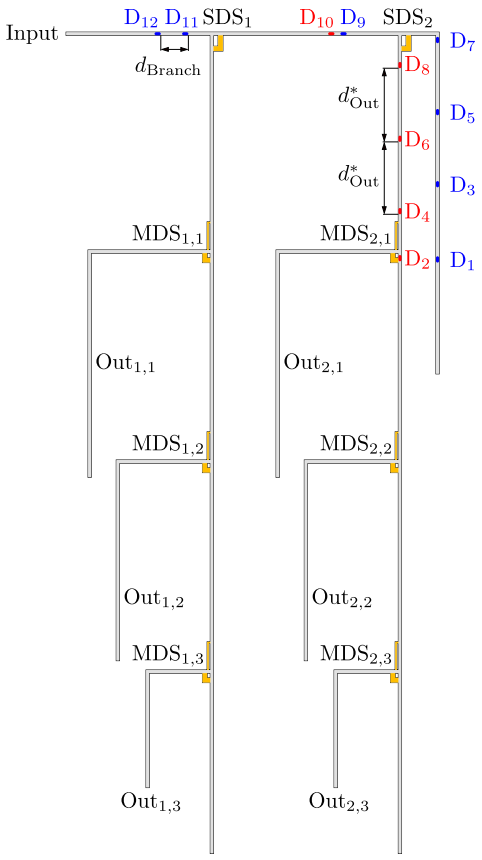

Fig. 17. Simulation screenshot of the MPDN.

VI. CONCLUSIONS

In this work, we proposed, for the first time, a passive droplet control scheme for two-dimensional microfluidic networks. In particular, we presented Single- and Multi-Payload-Droplet-Networks, which can route single and multiple payload droplets through distance-based addressing towards a specific destination, respectively. For both networks we specified the design conditions for the microfluidic switches, which were used to control the payload droplet path. Moreover, we characterized these switches by specific parameters, which were used to derive the required droplet distances that ensure the desired routing. Finally, we validated the proposed design of a Single- and Multi-Payload-Droplet-Network, using a simulator that is based on the analogy between microfluidic and electrical circuits.

VII. APPENDIX

A. Droplet Distances

As described in Section III-A2 and Section III-B2, the distance between two droplets (which flow towards a SDS or MDS) decides if the corresponding switching mechanism gets triggered or not. More precisely, if two droplets flow towards a SDS and their distance is shorter than a specific threshold d_{ON}, then the second droplet is routed into the non-default path of the SDS. In contrast, if the distance is longer than the threshold d_{OFF}, the second droplet follows the first one into the default path. For a MDS, the distance must lie between the thresholds

$d_{\text{ON,min}}$ and $d_{\text{ON,max}}$, if the switching mechanism should be triggered. If this should not happen, then the distance must be above the threshold d_{OFF}. In order to simplify the derivation of these thresholds, we first introduce a unified notation and some common parameters.

Basically, the thresholds can be derived by computing specific time intervals during the corresponding switching process, which depend on the passed distances and the velocities of the droplets. For example, the time interval $\Delta t_{1,0} = t_1 - t_0$ can be determined by

$$\Delta t_{1,0} = \frac{d_{\text{D1}}^{(\Delta t_{1,0})}}{v_{\text{D1}}^{(\Delta t_{1,0})}} \ , \tag{40}$$

where $d_{\text{D1}}^{(\Delta t_{1,0})}$ is the passed distance and $v_{\text{D1}}^{(\Delta t_{1,0})}$ the velocity of the droplet D_1 during the time interval $\Delta t_{1,0}$. Additionally, such a droplet velocity can always be described by a fraction of the input velocity

$$v_{\text{Input}} = \frac{Q_{\text{Input}}}{A} \ , \tag{41}$$

where Q_{Input} is the volumetric flow rate and A the cross section of the input channel. Furthermore, we assume, that all droplets have the same volume and, thus, the same length l_{Droplet}.

1) Threshold d_{ON} for a SDS: In order to derive the threshold d_{ON} for a SDS, we first look at Fig. 18a, which shows the moment t_0, when the first droplet D_1 has just entered the channel *In1* completely, while the second droplet D_2 still flows towards the SDS. Furthermore, we assume that the droplet distance at this time is $d = d_{\text{ON}}$, i.e. the value we want to derive. Since in this case the second droplet D_2 should be routed into the non-default path, the first droplet D_1 must still occupy the channel *In1*, when the second droplet arrives at the bifurcation point B_1. This particular moment is illustrated in Fig. 18b and represented by the time $t_1^{(\text{ON})}$. The corresponding time interval $\Delta t_{1,0} = t_1^{(\text{ON})} - t_0$ can be formulated as

$$\Delta t_{1,0} = \frac{d_{\text{D1}}^{(\Delta t_{1,0})}}{v_{\text{D1}}^{(\Delta t_{1,0})}} = \frac{d_{\text{D2}}^{(\Delta t_{1,0})}}{v_{\text{D2}}^{(\Delta t_{1,0})}} \ . \tag{42}$$

During this time interval the passed distances and the velocities of the two droplets can be described by

$$d_{\text{D1}}^{(\Delta t_{1,0})} = l_{\text{In1}} - l_{\text{Droplet}} \qquad v_{\text{D1}}^{(\Delta t_{1,0})} = q_{\text{In1}}^{(\text{In1})} v_{\text{Input}} \tag{43}$$

$$d_{\text{D2}}^{(\Delta t_{1,0})} = d_{\text{ON}} - l_{\text{Droplet}} \qquad v_{\text{D2}}^{(\Delta t_{1,0})} = v_{\text{Input}} \ , \tag{44}$$

where l_{In1} is the length and $q_{\text{In1}}^{(\text{In1})}$ the normalized volumetric flow rate of the channel *In1* (the superscript indicates, that a droplet is present inside the channel *In1*, as described in Section III-A1). When inserting (43) and (44) into (42) and rearranging the equation, the desired threshold can be computed as follows

$$d_{\text{ON}} = \frac{1}{q_{\text{In1}}^{(\text{In1})}} \left(l_{\text{In1}} - l_{\text{Droplet}} \right) + l_{\text{Droplet}} \ . \tag{45}$$

2) Threshold d_{OFF} for a SDS: For the derivation of the threshold d_{OFF}, we look at the initial moment t_0 again, which is sketched in Fig. 18a. However, this time we assume, that the droplet distance is $d = d_{\text{OFF}}$. In this scenario, the first

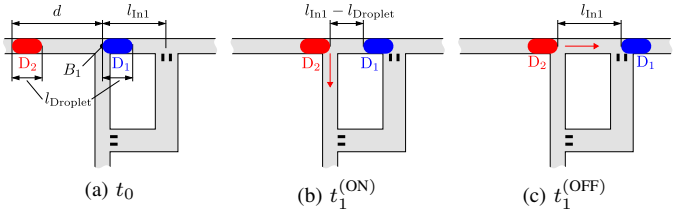

(a) t_0 (b) $t_1^{(\text{ON})}$ (c) $t_1^{(\text{OFF})}$

Fig. 18. Different time instances during the switching process.

droplet D_1 should not occupy the channel *In1* anymore, when the second droplet D_2 arrives at the bifurcation point B_1 and, thus, the second droplet should follow the first one into the default path. This specific moment is indicated by the time $t_1^{(\text{OFF})}$ and sketched in Fig. 18c. While the new time interval $\Delta t_{1,0} = t_1^{(\text{OFF})} - t_0$ can be formulated identical to (42), the passed distances and velocities of the two droplets change accordingly to

$$d_{\text{D1}}^{(\Delta t_{1,0})} = l_{\text{In1}} \qquad v_{\text{D1}}^{(\Delta t_{1,0})} = q_{\text{In1}}^{(\text{In1})} v_{\text{Input}} \tag{46}$$

$$d_{\text{D2}}^{(\Delta t_{1,0})} = d_{\text{OFF}} - l_{\text{Droplet}} \qquad v_{\text{D2}}^{(\Delta t_{1,0})} = v_{\text{Input}} \ . \tag{47}$$

Again, we can insert (46) and (47) into (42) and rearrange the equation, in order to get the desired threshold

$$d_{\text{OFF}} = \frac{1}{q_{\text{In1}}^{(\text{In1})}} l_{\text{In1}} + l_{\text{Droplet}} \ . \tag{48}$$

3) Threshold $d_{\text{ON,max}}$ for a MDS: In order to derive the threshold $d_{\text{ON,max}}$ for a MDS, we first look at Fig. 19a, which represents the initial moment t_0. That is, the first droplet D_1 has just entered the channel *C1*, while the second droplet D_2 still flows inside the input channel towards the MDS. Since we are searching the threshold $d_{\text{ON,max}}$, we assume, that the droplet distance at this time is $d = d_{\text{ON,max}}$. Because, in this scenario the MDS should be in the ON-State, the second droplet D_2 must block the control channel *Ctrl* when the first droplet D_1 arrives at the bifurcation point B_2. This is sketched in Fig. 19b (time $t_1^{(\text{ON,max})}$), where the second droplet just starts to block the control channel. The corresponding time interval $\Delta t_{1,0} = t_1^{(\text{ON,max})} - t_0$ can then be formulated identical to (42), with the following velocities and passed distances of the two droplets

$$d_{\text{D1}}^{(\Delta t_{1,0})} = l_{\text{C1}} - l_{\text{Droplet}} \qquad v_{\text{D1}}^{(\Delta t_{1,0})} = q_{\text{C1}}^{(\text{C1}),\,\text{OFF}} v_{\text{Input}} \tag{49}$$

$$d_{\text{D2}}^{(\Delta t_{1,0})} = d_{\text{ON,max}} - l_{\text{Droplet}} \qquad v_{\text{D2}}^{(\Delta t_{1,0})} = v_{\text{Input}} \ , \tag{50}$$

where l_{C1} is the length and $q_{\text{C1}}^{(\text{C1}),\,\text{OFF}}$ the normalized volumetric flow rate of the channel *C1* during the OFF-State (again, the superscript indicates, that a droplet is present inside the channel *C1*, as described in Section III-B1). After, inserting (49) and (50) into (42) and rearrange the equation, the desired threshold can be computed as follows

$$d_{\text{ON,max}} = \frac{1}{q_{\text{C1}}^{(\text{C1}),\,\text{OFF}}} \left(l_{\text{C1}} - l_{\text{Droplet}} \right) + l_{\text{Droplet}} \ . \tag{51}$$

4) Threshold $d_{\text{ON,min}}$ for a MDS: For the derivation of the threshold $d_{\text{ON,min}}$, we look, again, at Fig. 19a (time t_0), but this time, we assume, that the droplet distance is $d = d_{\text{ON,min}}$. In

this scenario, the second droplet D_2 starts to block the control channel *Ctrl* (cf. Fig. 19c at time $t_1^{(\mathrm{ON,min})}$) and, afterwards, just ends the clogging in the moment, when the first droplet D_1 arrives at the bifurcation point B_2 (cf. Fig. 19d at time $t_2^{(\mathrm{ON,min})}$). While the fist time interval $\Delta t_{1,0} = t_1^{(\mathrm{ON,min})} - t_0$ can be formulated identical to (42), the second time interval yields

$$\Delta t_{2,1} = t_2^{(\mathrm{ON,min})} - t_1^{(\mathrm{ON,min})} = \frac{d_{\mathrm{D1}}^{(\Delta t_{2,1})}}{v_{\mathrm{D1}}^{(\Delta t_{2,1})}} = \frac{d_{\mathrm{D2}}^{(\Delta t_{2,1})}}{v_{\mathrm{D2}}^{(\Delta t_{2,1})}} \ . \quad (52)$$

Moreover, the corresponding droplet velocities and the passed droplet distances can be formulated by

$$d_{\mathrm{D1}}^{(\Delta t_{1,0})} = ? \qquad v_{\mathrm{D1}}^{(\Delta t_{1,0})} = q_{\mathrm{C1}}^{(\mathrm{C1}),\,\mathrm{OFF}} v_{\mathrm{Input}} \quad (53)$$

$$d_{\mathrm{D2}}^{(\Delta t_{1,0})} = d_{\mathrm{ON,min}} - l_{\mathrm{Droplet}} \qquad v_{\mathrm{D2}}^{(\Delta t_{1,0})} = v_{\mathrm{Input}} \quad (54)$$

$$d_{\mathrm{D1}}^{(\Delta t_{2,1})} = ? \qquad v_{\mathrm{D1}}^{(\Delta t_{2,1})} = v_{\mathrm{Input}} \quad (55)$$

$$d_{\mathrm{D2}}^{(\Delta t_{2,1})} = l_{\mathrm{Droplet}} \qquad v_{\mathrm{D2}}^{(\Delta t_{2,1})} = v_{\mathrm{Input}} \ . \quad (56)$$

Please note, that the velocities of the two droplets during the time interval $\Delta t_{2,1}$ is the input velocity v_{Input}, because the second droplet D_2 blocks the control channel *Ctrl* during this time interval and, thus, the total flow rate flows inside the channel *C1*. As indicated, the values for $d_{\mathrm{D1}}^{(\Delta t_{1,0})}$, $d_{\mathrm{D1}}^{(\Delta t_{2,1})}$ are not known, but we know the sum of these two values, which is the total traveled distance of the first droplet D_1, yielding the following equation

$$d_{\mathrm{D1}}^{(\Delta t_{1,0})} + d_{\mathrm{D1}}^{(\Delta t_{2,1})} = l_{\mathrm{C1}} - l_{\mathrm{Droplet}} \ . \quad (57)$$

Now (53), (54), (55), and (56) can be inserted into (42) and (52). Afterwards, the three equations (42), (52), and (57) can be solved to get the desired threshold

$$d_{\mathrm{ON,min}} = \frac{1}{q_{\mathrm{C1}}^{(\mathrm{C1}),\,\mathrm{OFF}}} \left(l_{\mathrm{C1}} - 2 l_{\mathrm{Droplet}}\right) + l_{\mathrm{Droplet}} \ . \quad (58)$$

5) Threshold d_{OFF} for a MDS: We first consider Fig. 19a for the derivation of the threshold d_{OFF} and assume, that the distance between the droplets is now $d = d_{\mathrm{OFF}}$. In this scenario the first droplet D_1 completely passes the MDS, before the first droplet arrives at the bifurcation point B_1. Thus, the droplet D_1 flows through the channel *C1* until it arrives at the channel *In1*, as illustrated in Fig. 19e at time $t_1^{(\mathrm{OFF})}$. Afterwards, the droplet also passes the channel *In1* completely, before the second droplet arrives at the MDS (cf. Fig. 19f at time $t_2^{(\mathrm{OFF})}$). While the time intervals $\Delta t_{1,0} = t_1^{(\mathrm{OFF})} - t_0$ and $\Delta t_{2,1} = t_2^{(\mathrm{OFF})} - t_1^{(\mathrm{OFF})}$ can be formulated identical to (42) and (52), the passed distances and velocities of the two droplets change accordingly to

$$d_{\mathrm{D1}}^{(\Delta t_{1,0})} = l_{\mathrm{C1}} \qquad v_{\mathrm{D1}}^{(\Delta t_{1,0})} = q_{\mathrm{C1}}^{(\mathrm{C1}),\,\mathrm{OFF}} v_{\mathrm{Input}} \quad (59)$$

$$d_{\mathrm{D2}}^{(\Delta t_{1,0})} = ? \qquad v_{\mathrm{D2}}^{(\Delta t_{1,0})} = v_{\mathrm{Input}} \quad (60)$$

$$d_{\mathrm{D1}}^{(\Delta t_{2,1})} = l_{\mathrm{In1}} \qquad v_{\mathrm{D1}}^{(\Delta t_{2,1})} = q_{\mathrm{In1}}^{(\mathrm{In1}),\,\mathrm{OFF}} v_{\mathrm{Input}} \quad (61)$$

$$d_{\mathrm{D2}}^{(\Delta t_{2,1})} = ? \qquad v_{\mathrm{D2}}^{(\Delta t_{2,1})} = v_{\mathrm{Input}} \ . \quad (62)$$

Similar to before, the two distances $d_{\mathrm{D2}}^{(\Delta t_{1,0})}$ and $d_{\mathrm{D2}}^{(\Delta t_{2,1})}$ of the second droplet D_2 during the corresponding time intervals are not available, however, the total passed distance of the second droplet is known

$$d_{\mathrm{D2}}^{(\Delta t_{1,0})} + d_{\mathrm{D2}}^{(\Delta t_{2,1})} = d_{\mathrm{OFF}} - l_{\mathrm{Droplet}} \ . \quad (63)$$

Hence, after inserting (59), (60), (61), and (62) into (42) and (52), the three equations (42), (52), and (63) can be used again to determine the searched threshold

$$d_{\mathrm{OFF}} = \frac{l_{\mathrm{C1}}}{q_{\mathrm{C1}}^{(\mathrm{C1}),\,\mathrm{OFF}}} + \frac{l_{\mathrm{In1}}}{q_{\mathrm{In1}}^{(\mathrm{In1}),\,\mathrm{OFF}}} + l_{\mathrm{Droplet}} \ . \quad (64)$$

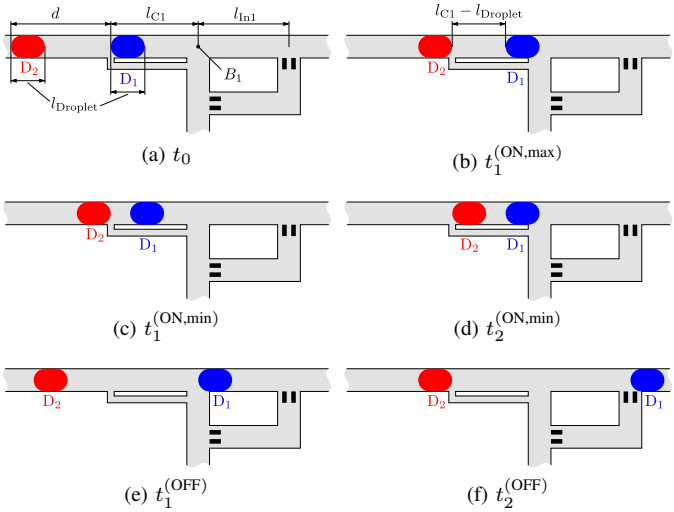

Fig. 19. Different time instances during the switching process

B. Droplet Distance Reduction

As mentioned in Section III-A3, if two droplets pass a SDS and flow into the same output channel, the distance between these droplets before and after the SDS is not identical, but reduces itself accordingly to the reduction factors r_1 or r_2 for the output channels *Out1* or *Out2*, respectively. The same scenario happens, when two droplets pass a MDS and flow towards the output channel *Out1*, as discussed in Section III-B3.

1) Reduction Factor r_1: In order to derive the reduction factor r_1 for the SDS and MDS (both denoted as *switch* in the following), we first look at Fig. 20, which shows four different time steps during this scenario. More precisely, the two droplets arrive at the switch with an initial distance of d_0 (cf. Fig. 20a at time t_0), then the first droplet D_1 passes the switch completely before the second droplet D_2 arrives at the switch (cf. Fig. 20b at time t_1). Afterwards, the second droplet also reaches the switch (cf. Fig. 20c at time t_2) and flows through it, until both droplets are present inside the output channel *Out1* and now have a droplet distance of d_3 (cf. Fig. 20d at time t_3). The reduction factor r_1 can then be described as $r_1 = d_3/d_0$.

As indicated in Fig. 20, the second droplet D_2 passes the distance d_0 during the time interval $\Delta t_{2,0} = t_2 - t_0$, whereas the first droplet D_1 travels the distance d_3 during the time interval $\Delta t_{3,1} = t_3 - t_1$. Moreover, the velocities of the droplets D_1 and D_2 during the corresponding time intervals

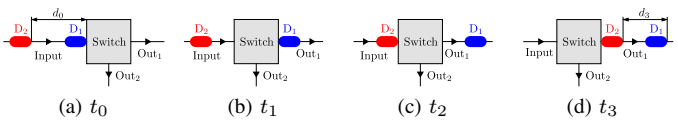

(a) t_0 (b) t_1 (c) t_2 (d) t_3

Fig. 20. Different time instances during the switching process

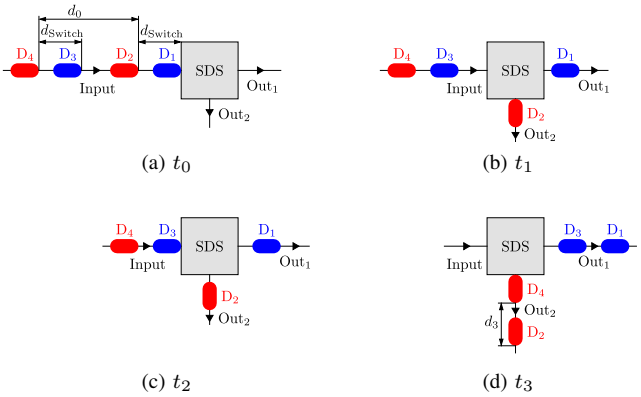

(a) t_0 (b) t_1 (c) t_2 (d) t_3

Fig. 21. Different moments during the switching process.

are $A/\left(q_{\text{Out1}}Q_{\text{Input}}\right)$ and A/Q_{Input}, respectively, where A is the channel cross-section, Q_{Input} the volumetric flow rate of the input channel, and q_{Out1} the normalized volumetric flow rate of the output channel *Out1*. As a result, the two time intervals can be formulated as

$$\Delta t_{2,0} = t_2 - t_0 = d_0 \frac{A}{Q_{\text{Input}}} \ , \tag{65}$$

$$\Delta t_{3,1} = t_3 - t_1 = d_3 \frac{A}{q_{\text{Out1}} Q_{\text{Input}}} \ . \tag{66}$$

Furthermore, we assume that the hydrodynamic resistances of the output channels are much larger than the other resistances, i.e, $R_{\text{Out1}}, R_{\text{Out2}} \gg R_{\text{In1}}, R_{\text{In2}}, R_{\text{By}}, R_{\text{Droplet}}$, which implies that the normalized volumetric flow rates of the output channels q_{Out1} and q_{Out2} are nearly constant. As a result, we can also assume, that both droplets need the same time to pass the switch, which leads to the following equation

$$\Delta t_{1,0} = t_1 - t_0 = t_3 - t_2 = \Delta t_{3,2} \ . \tag{67}$$

After rearranging (67) into the following form

$$\Delta t_{2,0} = t_2 - t_0 = t_3 - t_1 = \Delta t_{3,1} \ , \tag{68}$$

and inserting (65) and (66) we get

$$d_0 \frac{A}{Q_{\text{Input}}} = d_3 \frac{A}{q_{\text{Out1}} Q_{\text{Input}}} \ . \tag{69}$$

With this equation, the reduction factor can now be easily computed by

$$r_1 = \frac{d_3}{d_0} = q_{\text{Out1}} \ . \tag{70}$$

That is, the reduction factor r_1 is just the value of the normalized volumetric flow rate q_{Out1}, which, of course, depends on the used switch and can be found in the corresponding Secs. III-A3 (for the SDS) and III-B3 (for the MDS).

2) Reduction Factor r_2: The reduction factor r_2 for a SDS can be derived similar to the reduction factor r_1, however, since this time two droplets must be routed into the channel *Out2*, two additional droplets are needed to trigger the switching process of the SDS. Hence, as indicated in Fig. 21, the droplets D_1 and D_3 are responsible to route the corresponding droplets D_2 and D_4 into the non-default path. Therefore, we assume, that the distance between the droplets D_1 and D_2 and between the droplets D_3 and D_4 is identical, namely d_{Switch}, and has such a value, that the switching mechanism of the SDS gets triggered. In contrast, the initial distance between the droplets D_2 and D_4 is d_0 (cf. Fig. 21a at time t_0). After the droplets D_1 and D_2 have passed the switch (cf. Fig. 21b at time t_1), the droplets D_3 and D_4 arrive at the entrance of the switch (cf. Fig. 21c at time t_2). At time t_3, all droplets have already passed the switch, where the droplets D_1 and D_3 are present inside the output channel *Out1*, while the droplets D_2 and D_4 flow inside the channel *Out2* and now have a reduced distance of d_3. Hence, the reduction factor r_2 can, again, be formulated by $r_2 = d_3/d_0$.

Like above, the time intervals $\Delta t_{2,0}$ and $\Delta t_{3,1}$ can be described with the help of the passed distances and the velocities of the droplets D_4 (distance d_0 and velocity A/Q_{Input}) and D_2 (distance d_3 and velocity $A/\left(q_{\text{Out2}}Q_{\text{Input}}\right)$)

$$\Delta t_{2,0} = t_2 - t_0 = d_0 \frac{A}{Q_{\text{Input}}} \ , \tag{71}$$

$$\Delta t_{3,1} = t_3 - t_1 = d_3 \frac{A}{q_{\text{Out2}} Q_{\text{Input}}} \ . \tag{72}$$

Again, we assume that the hydrodynamic resistances of the output channels are much larger than the other resistances, resulting in nearly constant values of q_{Out1} and q_{Out2}. As a result, the droplet pair D_1 and D_2 and the droplet pair D_3 and D_4 need the same time to pass the SDS, which yields the same equation as (67) and can also be rearranged to match (68). Hence, after inserting (71) and (72) into (68), we get

$$d_0 \frac{A}{Q_{\text{Input}}} = d_3 \frac{A}{q_{\text{Out2}} Q_{\text{Input}}} \ . \tag{73}$$

This equation can then be used to derive the desired reduction factor

$$r_2 = \frac{d_3}{d_0} = q_{\text{Out2}} = 1 - q_{\text{Out1}} \ , \tag{74}$$

where the last simplification can be made due to Kirchhoff's current law ($q_{\text{Out1}} + q_{\text{Out2}} = 1$). How to compute the value for q_{Out1} can be found in Section III-A3.

Please note, that the reduction factor r_2 for a MDS is not needed in this work and, thus, its derivation is not discussed here. However, it would also be possible to determine this factor, despite the fact, that a few more aspects have to be considered due to the working principles of the MDS.

REFERENCES

[1] N. Farsad, H. B. Yilmaz, A. Eckford, C. B. Chae, and W. Guo, "A comprehensive survey of recent advancements in molecular communication," *IEEE Commun. Surveys Tuts.*, vol. 18, no. 3, pp. 1887–1919, thirdquarter 2016.

[2] P. He, Y. Mao, Q. Liu, P. Liò, and K. Yang, "Channel modelling of molecular communications across blood vessels and nerves," in *Proc. IEEE Int. Conf. Communications*, May 2016, pp. 1–6.

[3] A. O. Bicen, J. J. Lehtomäki, and I. F. Akyildiz, "Shannon meets Fick on the microfluidic channel: Diffusion limit to sum broadcast capacity for molecular communication," *IEEE Trans. Nanobiosci.*, vol. 17, no. 1, pp. 88 – 94, Mar. 2018.

[4] A. O. Bicen and I. F. Akyildiz, "End-to-end propagation noise and memory analysis for molecular communication over microfluidic channels," *IEEE Trans. Commun.*, vol. 62, no. 7, pp. 2432–2443, July 2014.

[5] W. Wicke, T. Schwering, A. Ahmadzadeh, V. Jamali, A. Noel, and R. Schober, "Modeling duct flow for molecular communication," in *Proc. IEEE Global Commmunications Conf.*, Dec 2018, pp. 206–212.

[6] Y. Sun, K. Yang, and Q. Liu, "Channel capacity modelling of blood capillary-based molecular communication with blood flow drift," in *Proc. Int. Conf. Nanoscale Computing and Communication*, ser. NanoCom '17. New York, NY, USA: ACM, 2017, pp. 19:1–19:6. [Online]. Available: http://doi.acm.org/10.1145/3109453.3109454

[7] N. Varshney, W. Haselmayr, and W. Guo, "On flow-induced diffusive mobile molecular communication: First hitting time and performance analysis," *Trans. on Molecular, Biological, and Multi-scale Communications*, vol. 4, no. 4, pp. 195–207, 2018.

[8] E. De Leo, L. Galluccio, A. Lombardo, and G. Morabito, "Networked labs-on-a-chip (NLoC): Introducing networking technologies in microfluidic systems," *Nano Communication Networks*, vol. 3, no. 4, pp. 217–228, 2012.

[9] E. De Leo, L. Donvito, L. Galluccio, A. Lombardo, G. Morabito, and L. M. Zanoli, "Communications and switching in microfluidic systems: Pure hydrodynamic control for networking Labs-on-a-Chip," *Trans. on Communications*, vol. 61, no. 11, pp. 4663–4677, 2013.

[10] M. Hamidović, , U. Marta, G. Fink, R. Wille, A. Springer, and W. Haselmayr, "Information encoding in droplet-based microfluidic systems: First practical study," in *Proc. Int. Conf. Nanoscale Computing and Communications*, Sept 2019, pp. 1–6.

[11] L. Galluccio, A. Lombardo, G. Morabito, S. Palazzo, C. Panarello, and G. Schembra, "Capacity of a binary droplet-based microfluidic channel with memory and anticipation for flow-induced molecular communications," *IEEE Trans. Commun.*, vol. 66, no. 1, pp. 194–208, Jan 2018.

[12] W. Haselmayr, A. Grimmer, and R. Wille, "Stochastic computing using droplet-based microfluidics," in *Proc. Computer Aided Systems Theory*, R. Moreno-Díaz, F. Pichler, and A. Quesada-Arencibia, Eds. Cham: Springer International Publishing, 2018, pp. 204–211.

[13] L. Donvito, L. Galluccio, A. Lombardo, and G. Morabito, "μ-NET: A network for molecular biology applications in microfluidic chips," *IEEE/ACM Transactions on Networking (TON)*, vol. 24, no. 4, pp. 2525–2538, 2016.

[14] W. Haselmayr, A. Biral, A. Grimmer, A. Zanella, A. Springer, and R. Wille, "Addressing multiple nodes in networked labs-on-chips without payload re-injection," in *Proc. IEEE Global Commmunications Conf.*, May 2017, pp. 1–6.

[15] W. Haselmayr, M. Hamidović, A. Grimmer, and R. Wille, "Fast and flexible drug screening using a pure hydrodynamic droplet control," in *Proc. Euro. Conf. Microfluidics*, 2018, pp. 1–4.

[16] M. Hamidović, W. Haselmayr, A. Grimmer, R. Wille, and A. Springer, "Passive droplet control in microfluidic networks: A survey and new perspectives on their practical realization," *Nano Communication Networks*, 2018.

[17] G. Castorina, M. Reno, L. Galluccio, and A. Lombardo, "Microfluidic networking: Switching multidroplet frames to improve signaling overhead," *Nano Communication Networks*, vol. 14, pp. 48–59, 2017.

[18] A. Zanella and A. Biral, "Design and analysis of a microfluidic bus network with bypass channels," in *2014 IEEE International Conference on Communications (ICC)*. IEEE, 2014, pp. 3993–3998.

[19] G. Fink, M. Hamidović, W. Haselmayr, and R. Wille, "Automatic design of droplet-based microfluidic ring networks."

[20] A. Grimmer, W. Haselmayr, A. Springer, and R. Wille, "Design of application-specific architectures for Networked Labs-on-Chips," *Trans. on Computer-Aided Design of Integrated Circuits and Systems*, vol. 37, no. 1, pp. 193–202, 2018.

[21] A. Lombardo, G. Morabito, and M. Reno, "Cabling DNA-based archival storage systems through microfluidic networks," in *2017 European Conference on Circuit Theory and Design (ECCTD)*. IEEE, 2017, pp. 1–4.

[22] J. Bornholt, R. Lopez, D. M. Carmean, L. Ceze, G. Seelig, and K. Strauss, "A DNA-based archival storage system," in *Proceedings of the Twenty-First International Conference on Architectural Support for Programming Languages and Operating Systems*, 2016, pp. 637–649.

[23] A. Grimmer, X. Chen, M. Hamidović, W. Haselmayr, C. L. Ren, and R. Wille, "Simulation before fabrication: a case study on the utilization of simulators for the design of droplet microfluidic networks," *RSC Adv.*, vol. 8, pp. 34 733–34 742, 2018. [Online]. Available: http://dx.doi.org/10.1039/C8RA05531A

[24] A. Grimmer, M. Hamidović, W. Haselmayr, and R. Wille, "Advanced simulation of droplet microfluidics," *Journal on Emerging Technologies in Computing Systems*, 2019.

[25] K. W. Oh, K. Lee, B. Ahn, and E. P. Furlani, "Design of pressure-driven microfluidic networks using electric circuit analogy," *Lab on a Chip*, vol. 12, no. 3, pp. 515–545, 2012.

[26] A. Grimmer, W. Haselmayr, and R. Wille, "Automated dimensioning of Networked Labs-on-Chip," *Trans. on Computer-Aided Design of Integrated Circuits and Systems*, 2018.

[27] H. Bruus, *Theoretical microfluidics*. Oxford university press Oxford, 2008, vol. 18.

[28] M. J. Fuerstman, A. Lai, M. E. Thurlow, S. S. Shevkoplyas, H. A. Stone, and G. M. Whitesides, "The pressure drop along rectangular microchannels containing bubbles," *Lab on a Chip*, vol. 7, no. 11, pp. 1479–1489, 2007.

[29] T. Glawdel and C. L. Ren, "Global network design for robust operation of microfluidic droplet generators with pressure-driven flow," *Microfluidics and Nanofluidics*, vol. 13, no. 3, pp. 469–480, 2012.

[30] A. Biral and A. Zanella, "Introducing purely hydrodynamic networking functionalities into microfluidic systems," *Nano Communication Networks*, vol. 4, no. 4, pp. 205–215, 2013.

[31] L. Donvito, L. Galluccio, A. Lombardo, and G. Morabito, "Microfluidic networks: Design and simulation of pure hydrodynamic switching and medium access control," *Nano Communication Networks*, vol. 4, no. 4, pp. 164–171, 2013.

[32] G. Cristobal, J.-P. Benoit, M. Joanicot, and A. Ajdari, "Microfluidic bypass for efficient passive regulation of droplet traffic at a junction," *Applied Physics Letters*, vol. 89, no. 3, pp. 34 104–34 104, 2006.

[33] A. Biral, D. Zordan, and A. Zanella, "Modeling, simulation and experimentation of droplet-based microfluidic networks," *Trans. on Molecular, Biological, and Multi-scale Communications*, vol. 1, no. 2, pp. 122–134, 2015.

[34] X. Chen and C. L. Ren, "A microfluidic chip integrated with droplet generation, pairing, trapping, merging, mixing and releasing," *RSC Advances*, vol. 7, no. 27, pp. 16 738–16 750, 2017.

Gerold Fink received the Master's degree in mechatronics from the Johannes Kepler University Linz, Austria, in 2019. Currently, he is a Ph.D. student at the Institute of Integrated Circuits at the Johannes Kepler University. His research area focuses on simulations and design automations for microfluidic networks.

Medina Hamidović has received her B.Sc. degree in electrical engineering at the University of Tuzla in 2014. In 2017, Hamidović received her joint Master's degree in electrical engineering from Heriot-Watt University (UK), University of South-East Norway and Budapest University of Technology and Economics. At the moment, Hamidović is a Ph.D. researcher at the Institute for Communications Engineering and RF-Systems at the Johannes Kepler University Linz (Austria). Her research is focused on the area of molecular communications and microfluidic networks.

Rober Wille (M'06–SM'15) is Full Professor at the Johannes Kepler University Linz, Austria. He received the Diploma and Dr.-Ing. degrees in Computer Science from the University of Bremen, Germany, in 2006 and 2009, respectively. Since then, he worked at the University of Bremen, the German Research Center for Artificial Intelligence (DFKI), the University of Applied Science of Bremen, the University of Potsdam, and the Technical University Dresden. Since 2015, he is working in Linz. His research interests are in the design of circuits and systems for both conventional and emerging technologies. In these areas, he published more than 300 papers in journals and conferences and served in editorial boards and program committees of numerous journals/conferences such as TCAD, ASP-DAC, DAC, DATE, and ICCAD. For his research, he was awarded, e.g., with a Best Paper Award at ICCAD, a DAC Under-40 Innovator Award, a Google Research Award, and more.

Werner Haselmayr (S'08–M'13) is an Assistant Professor at the Institute for Communications Engineering and RF-Systems, Johannes Kepler University Linz, Austria. He received the Ph.D. degree in mechatronics from the same university in 2013. His research interests include the design and analysis of synthetic molecular communication systems and communications and networking in droplet-based microfluidic systems. He has given several invited talks and tutorials on various aspects of droplet-based communications and networking. He has authored 2 book chapters and more than 60 papers, appeared in top-level international peer-reviewed journals and conference proceedings. Currently, he serves as Associate Editor for the IEEE Transactions on Molecular, Biological, and Multi-Scale Communications.